IMPACT TEST SIMULATION OF CAR ROOF USING FINITE ELEMENT ANALYSIS (FEA)

GAN YEE HOE

UNIVERSITI TEKNIKAL MALAYSIA MELAKA

IMPACT TEST SIMUALTION OF CAR ROOF USING FINITE ELEMENT ANALYSIS (FEA)

GAN YEE HOE

A report submitted in fulfilment of the requirement for the degree of Bachelor of Mechanical Engineering (Hons)

Faculty of Mechanical Engineering

UNIVERSITI TEKNIKAL MALAYSIA MELAKA

2019

DECLARATION

I declare that this project entitled “Impact Test Simulation of Car Roof Using Finite Element Analysis (FEA)” is the result of my own work except as cited in the references.

Signature : ……………………………………..

Name : ………………………….……………

Date : ………………………….……………

APPROVAL

I hereby declare that I have read this project report and in my opinion this report is sufficient in term of scope and quality for the award of the degree of Bachelor of Mechanical Engineering (Hons).

Signature : ……………………………………
Name of supervisor : ……………………………………
Date : ……………………………………

DEDICATION

To my beloved mother and father

ABSTRACT

For present, it seems that most of the crash studies and New Car Assessment Program (NCAP) existed worldwide focused mainly on frontal impact, side impact and roof strength test. When a crash involves a large truck and passenger vehicle, the occupants of the smaller vehicle is more likely to be injured or fatal. This is because two impacting vehicles; large truck and passenger vehicle are geometrically mismatch as the bottom of the truck is higher than car hood. This type of crashes is known as underride crash because passenger vehicle usually slides under the large truck during the crash. This condition bypasses the crumple zone of the passenger vehicle and no impact energy can be absorbed. The energy absorption of impact energy will be solely depending on the strength of roof pillars. In existing roof strength test, roof crush in rollover accident is simulated. However, roof strength test involve impact on each side of the car roof to simulate underride accident is virtually absent. Therefore, the objectives of this project are to improve the design of 3D model of car roof based on PROTON WIRA using CATIA software and to determine the energy absorbed on different side of car roof (front, rear, side) during the impact. Real car roof structure is measured and modelled into 3D model using CATIA software and exported to ABAQUS to carry out impact test simulation using finite element analysis (FEA). Three impact test simulation are conducted; frontal impact test, side impact test and rear impact test using an impactor of weight 16000kg. Each type of simulation is conducted with two different impact velocity; 80km/h and 90km/h to study the relationship between energy absorbed and impact velocity. In addition, mesh sensitivity analysis is performed for each of the simulation by using five different mesh size of car roof structure; 85mm, 60mm, 40mm, 30mm and 20mm. Therefore, there are a total number of 30 simulations conducted in which each type of impact test consists of 10 simulations with 5 simulations each for a single impact velocity. From the results of this project, it shows that the energy absorbed by the car roof structure is increase with impact velocity for all type of impact. In addition, the energy absorption capability is in an increasing order for B-pillar (side impact) to A-pillars (frontal impact) to C-pillars (rear impact). The significance of the result from this project is able to identify the strength of car roof in different orientation. Further research on energy absorption capability can be done by using different materials or even different design of car roof pillars. By enhancing the crashworthiness of the car roof structure, fatality involved in underride crash can be reduced and save precious life.

ABSTRAK

Buat masa ini, nampaknya kebanyakan kajian kemalangan dan Program Penilaian Kereta Baharu (NCAP) yang wujud di seluruh dunia memberi tumpuan utama pada ujian pelanggaran dari hadapan, ujian pelanggaran dari sisi dan ujian kekuatan bumbung. Apabila kemalangan melibatkan lori besar dan kenderaan penumpang, penumpang yang berada di kenderaan kecil sering mengalami kecederaan atau kematian. Ini kerana bahagian bawah lori besar adalah lebih tinggi daripada bonet depan kenderaan penumpang. Jenis kemalangan ini dikenali sebagai "underride crash" kerana kenderaan penumpang biasanya meluncur ke bawah lori apabila merempuh laju dengan lori. Penyerapan tenaga impak akan semata-mata bergantung kepada kekuatan bumbung kereta kerana bonet kereta yang direka cipta khas untuk menyerap tenaga semasa pelanggaran telah pun dilepasi. Dalam ujian kekuatan bumbung kenderaan yang sedia ada, kemalangan "rollover" disimulasikan. Walau bagaimanapun, ujian kekuatan bumbung kenderaan yang melibatkan pelanggaran dari setiap sisi bumbung kereta untuk mensimulasikan kemalangan "underride crash" ini adalah hampir tidak hadir. Oleh itu, objektif projek ini adalah untuk mereka bentuk model 3D bumbung kereta berdasarkan kereta PROTON WIRA menggunakan perisian CATIA dan untuk menentukan tenaga yang diserap oleh bumbung kereta di bahagian yang berlainan (depan, belakang, sebelah) semasa impak. Struktur bumbung kereta sebenar telah diukur dan dimodelkan ke dalam model 3D menggunakan perisian CATIA dan dieksport ke perisian ABAQUS untuk menjalankan simulasi ujian impak menggunakan analisis unsur terhingga (FEA). Tiga jenis simulasi ujian impak telah dijalankan; ujian impak hadapan, ujian impak sisi dan ujian impak belakang dengan mengunnakan 16000kg model lori. Setiap jenis simulasi ujian impak dijalankan dengan dua halaju impak yang berlainan; 80km/j dan 90km/j untuk mengkaji hubungan antara tenaga yang diserap dan halaju impak. Di samping itu, analisis kepekaan mesh dilakukan untuk setiap jenis simulasi ujian impak dengan menggunakan lima saiz mesh yang berlainan untuk struktur bumbung kereta; 85mm, 60mm, 40mm, 30mm dan 20mm. Sejumlah 30 simulasi telah dijalankan di mana setiap jenis ujian impak terdiri daripada 10 simulasi dengan 5 simulasi untuk setiap halaju impak. Dari hasil projek ini, ia menunjukkan bahawa tenaga yang diserap oleh struktur bumbung kereta meningkat dengan halaju impak untuk setiap jenis ujian impak. Di samping itu, keupayaan penyerapan tenaga meningkat dari B-pillar (ujian impak sisi) kepada A-pillars (ujian impak hadapan) kepada C-pillars (ujian impak belakang). Kepentingan hasil daripada projek ini adalah dapat mengenal pasti kekuatan bumbung kereta dalam orientasi yang berbeza. Kajian lanjut mengenai keupayaan penyerapan tenaga boleh dilakukan dengan menggunakan bahan yang berbeza ataupun reka bentuk bumbung kereta yang berbeza. Dengan meningkatkan kecekapan struktur bumbung kereta, kematian yang terlibat dalam kemalangan "underride crash" ini dapat dikurangkan dan mampu menyelamatkan nyawa yang berharga.

ACKNOWLEDGEMENTS

First and foremost, I would like to take this opportunity to express my deepest appreciation to my supervisor, Dr. Mohd Basri Bin Ali from the Faculty of Mechanical Engineering Universiti Teknikal Malaysia Melaka (UTeM) for his continuous support, encouragement and motivation to coordinate my project especially in writing this report.

Furthermore, I would like to thank Mr. Hairul Bin Bakri bin Ali and Profesor Madya Dr Mohd Ahadlin Bin Mohd Daud for giving me more ideas and suggestions to improve the design of 3D model of car roof structure. They are willing to share their engineering knowledge, gave some advice for the analysis work during the PSM seminar.

My sincerely thanks also go to my parents, siblings and friends for their moral support in completing this degree. Lastly, I would like to thank you to everyone who had been spending their precious time to assist me to finish this project successfully.

TABLE OF CONTENTS

LIST OF TABLES

LIST OF FIGURES

LIST OF APPENDICES

LIST OF ABBREVIATIONS

MOT	MINISTRY OF TRANSPORT
MIROS	Malaysian Institute of Road Safety Research
NCAP	New Car Assessment program
FMVSS	Federal Motor Vehicle Safety Standard
RSPM	Road Safety Plan of Malaysia
FEA	Finite Element Analysis
PCI	Passenger Compartment Intrusion
NHTSA	National Highway Traffic Safety Administration
IIHS	Insurance Institute for Highway Safety
ESC	Electronic Stability Control
FARS	Fatality Analysis Reporting System

CHAPTER 1

INTRODUCTION

1.1 Background

In recent years, Association of Southeast Asian Nations (ASEAN) countries rising rapidly in term of population and economy. The increase in population of these countries has contributed to the growth of motorization significantly. This situation has led to an alarming increase of the road accidents. In ASEAN region, accidents involving 4-wheels vehicles come second after vulnerable road users in low and middle income countries (Mohd Syazwan *et al.*, 2014).

The rates of road accident that cause the death in Malaysia recorded high each year, wherein 2011 is 6877, in 2012 is 6917, in 2013 is 6915 and 6674 in 2014. From the latest accident statistics from the database of MINISTRY OF TRANSPORT (MOT), Number of deaths in 2015 is 6706 and in 2016 is 7152. Although the Index of road accident fatalities per 10,000 registered vehicles (index of deaths) have been decreased from 3.21 in 2011 to 2.59 in 2016, this still contrasts with fatality rates of less than 2 per 10,000 registered vehicles in developed countries. Based on statistics, motorist ranked second with fatalities form accident which is just below motorcyclist fatalities in Malaysia (Ministry Of Transport Malaysia).

The Road Safety Plan of Malaysia 2014-2020 (RSPM 2014-2020) has been created to address all matters related to road safety in the country to achieve our common vision to minimise road accidents, injuries and fatalities by the year 2020 based on Five Strategic Pillars. Strategic pillar 3 in the framework of Road Safety Plan of Malaysia 2014-2020 is about safer vehicles. Under strategic pillar 3, Midterm outcome (MO6) is about Improvements in crashworthiness requirements for new vehicles (Road Safety Department and Malaysian Institute of Road Safety Research, 2014). Over the past decades, more concerns had given to the crashworthiness and safety of road vehicles. A lot of researches rose in mid-90s, when occupant safety established itself as an essential characteristics of motor vehicles. Structural elements which are lighter and more deformable became the important factor to improve crashworthiness of the vehicles (Costas *et al.*, 2013).

Malaysia took its own initiative to enhance road safety situation in the country by established a research and development agency known as the Malaysian Institute of Road Safety Research (MIROS). In the period between 2008-2011, MIROS had established its own capacity to conduct crash testing and created a rating program called Malaysian Vehicle Assessment Program (MyVAP) (Jawi, Kassim and Sadullah, 2013). In 2011, ASEAN NCAP was established by MIROS and Global NCAP to make sure automobile manufacturer did not risk on car occupants' safety in ASEAN region (Mohd Syazwan *et al.*, 2014). A full-scale crash lab was developed by MIROS and operated since May 2012 onwards. The destructive assessment method, full scale crash test replaced the non-destructive method of safety assessment called Malaysian Vehicle Assessment Programme (MyVAP). NCAP star rate new cars based on its safety performance through crash test and aids consumer to choose safer car (Road Safety Department and Malaysian Institute of Road Safety Research, 2014).

Frontal crashes produce nowadays 50-70% of the fatalities by car accidents (Costas *et al.*, 2013), whereas the side impacts account for approximately 30% of all impacts and 35% of total fatalities. (Njuguna, 2011). Rollover crashes are less common than frontal, side, or rear impact collisions but it causes higher risk of injury and fatality compare to other crash type (Dobbertin *et al.*, 2013). Roof strength will affects the risk of occupant head and neck injury in car rollovers (Friedman and CE, 2001). Deaths and a large majority of the injuries in rollover crashes can be eliminated if the car roof structure is strong and the occupants are restrained by a three point seat belt (Grzebieta, Mcintosh and Simmons, 2012).

There are different types of static and dynamic roof crush tests in worldwide such as the Federal Motor Vehicle Safety Standard (FMVSS) 216, Inverted Vehicle Drop Dynamic Test (Society of Automotive Engineering, SAE, J996) and Dolly Rollover Test (SAE J2114) that are aimed to evaluate the vehicle roof structure performance (Borazjani and Belingardi, 2017).

1.2 Problem Statement

By the end of Road Safety Plan of Malaysia (RSPM) 2014-2020, the number of road fatalities is to be reduced to 5,358 from the predicted number of 10,716 in 2020. To ensure that the target of RSPM 2014-2020 is met, the RSPM 2014-2020 will be implemented through five Strategic Pillars. (Road Safety Department and Malaysian Institute of Road Safety Research, 2014). For this project, we will focus on the pillar 3, which is safer vehicles and we further focus on midterm outcome, MO6 - Improvements in crashworthiness requirements for new vehicles. Under the programme of safety performance evaluation in the RSPM 2014-2020, ASEAN NCAP will conduct a crash test on new cars and give star rate based on the result obtained (Road Safety Department and Malaysian Institute of Road Safety Research, 2014). When first established in 2011, ASEAN NCAP only performs one crash test which is frontal offset test (Jawi, Kassim and Sadullah, 2013). In September 2015, ASEAN NCAP introduced the new rating scheme for 2017-2020 which included more crash test such as full-wrap frontal test and side impact test (ASEAN NCAP, 2017).

For this project, focus is on the type of crash test but not the crash avoidance technologies such as Electronic Stability Control (ESC) and Seatbelt Reminder (SBR). Currently, it seems that most of the crash studies and New Car Assessment program existed worldwide focused mainly on frontal impact and side impact and roof strength test (FMVSS No. 216). For FMVSS No. 216 test, roof crush in rollover accident is simulated.

When a crash involves of a large truck and a passenger vehicle, the occupants of the smaller vehicle is more likely to be injured or fatal. About 94% of the fatalities of this kind of accident is represented by occupants of the smaller vehicles, whereas 6% only represented by occupants of the truck (U.S. Department of Transportation [USDOT], 2001). This type of crashes is known as underride. When a motor vehicle slides at least partially under a large truck during a crash, it can be defined as underride crash. Underride crash increase the passenger compartment which will be intruded into the truck significantly, this will escalate the risk of injury or fatality of the occupants of the smaller vehicle that crashes into the heavy truck (Roberts and Lynn, 2003). Figure 1.1 and Figure 1.2 show the side underride and rear end underride crash respectively.

Figure 1.1: A car crash into side of a truck (www.today.com)

Figure 1.2: Rear-end underride crash (www.autosafetyexpert.com)

However, roof strength test involve impact on each side of the car roof to simulate this kind of crashes is virtually absent. Almost no previous scientific studies involve side impact on the car roof which on the front, rear, right and left when this kind of accidents happened involved of a smaller vehicle and a heavy vehicle. Therefore, the purpose of this project is to investigate the role of car roof in underride crash and study the roof strength in terms of energy absorbed by the car roof in the directions as shown in Figure 1.3 during the underride accident.

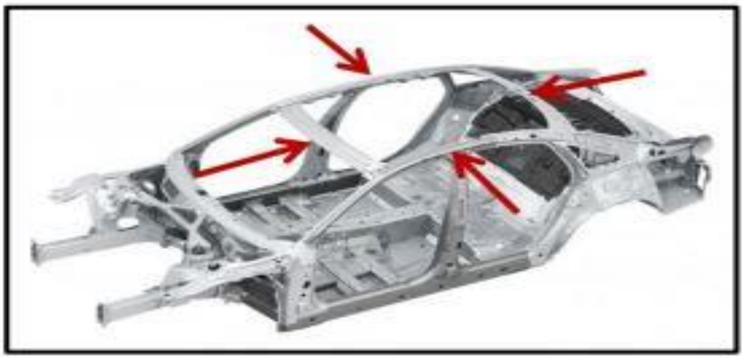

Figure 1.3: The directions of impact on the car roof in the impact test simulation of this project (MUHAMMAD AFIFUDDIN, 2018)

1.3 Objectives

The objectives of this project are as follows:

1. To improve the design of 3D model for real car roof by adding body structure to the car roof.
2. To determine the energy absorbed on different side of car roof (front, rear, side) during the impact.

1.4 Scopes of Project

The scopes of this project are listed as below:

1. The design of the 3D model of car roof based on PROTON WIRA using CATIA software.
2. The Finite Element Analysis (FEA) of the project will be carried out by using ABAQUS software.

CHAPTER 2

LITERATURE REVIEW

2.1 Overview

This chapter reviews the introduction to car roof, background and the type of impact test of vehicles, energy absorption during a crash and finite element analysis.

2.2 Car Roof

A car roof (also known as car top) isolates occupant from external environment such as sun and rain. There are pillars made up the part of body structure which supports the car roof as shown in Figure 2.1. The forward most roof pillar is known as A pillar which dividing car's front windscreen from front side window, the centre side door pillar is known as B pillar and lastly the third roof pillar is known as C pillar which dividing car's rear window from rear windscreen. In bigger car such as SUV which have larger cargo areas, it has an extra pillar called D-pillar. Strong roof and roof pillars can provide more protection to the car's occupants by reducing the passenger compartment intrusion (PCI) during a crash.

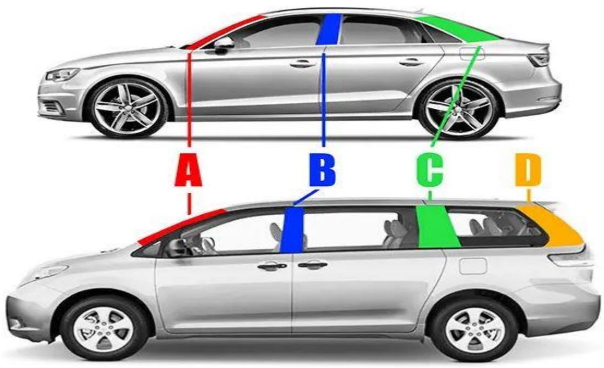

Figure 2.1: Roof pillars that support the car roof (Wishdom, 2018)

2.3 Impact

Impact occurs when a moving body collide with another body which it is either at rest or in motion. The time taken for the impact to happen is usually very short. During the impact, the two colliding bodies impose forces on each other (Zainuddin *et al.*, 2016)

Impact also known as collision. There are two types of collision which are elastic and inelastic collision. In elastic collision, two body come to impact will bounce off each other with no loss in speed because no energy is lost. In inelastic collision, objects colliding stick together after impact and lost kinetic energy through sound, heat and material deformation (Zainuddin *et al.*, 2016).

In an impact of vehicles, if the collision happens in low speed, it is an elastic collision. Bumper of car prevent damage by deform and then bounce back in a low speed collision. This process transfers all the energy back into motion and almost no energy is converted into heat, noise, or deformation of the car. If impact happens in high speed, it is an inelastic collision that dissipate big amount of energy through material deformation of the vehicles and some kinetic energy loss through noise and heat (*Types of Collisions*, 2018).

2.3.1 Mechanism of Car Impact

Newton's Law of Motion is governing the car impacts. Newton's first law of motion which also known as law of inertia, implies that the moving vehicle will keep on moving unless an external force acting on it. Therefore, the moving vehicle will continue to move until it collides with another vehicle or any object and stop completely. Upon the collision, force generated is defined by Newton's second law of motion which stated that force is equals to mass multiply by acceleration. For impact case, the acceleration is the measure of deceleration of the car from initial travelling velocity to zero velocity . The shorter the time taken for it to come stop completely, the greater the acceleration and hence a greater force is generated by the striking car.

For the first scenario, where the car crash to a rigid body which is not deformable such as rigid wall, the car exerts this force in the direction of wall. Newton's Third law of motion implies that this wall will impose an equal magnitude of force back on the car (*Types of Collisions*, 2018).

For the second scenario, where the car collides with another moving vehicle, the force generated is different from first scenario. A high-speed car collision is a type of inelastic collision where the vehicles does not bounce off each other but they stuck to each other and move together with a same velocity until a stop during the impact. In inelastic collision, momentum is conserved but kinetic energy is not. The force experienced by the cars are depending on the mass of the striking vehicle and its own acceleration. Initially, each car has own kinetic energy depending on its own mass and moving velocity. After the collision, total kinetic energy of the system become zero because both vehicles stop completely. This implies that the kinetic energy is lost by convert into other energy form such as heat, sound and deformation of objects. In this type of impact, energy generated is total of the energy released by both vehicles (Physics and Collision, 2018)

2.3.2 Impact Test

Since the early 1900, Crash testing has been created due to the number of vehicles on the road has escalated to a level that accidents started to occur frequently. Crash tests are a method of securing the public safety. In the automotive industry, impact tests between cars are conducted to study the damage caused by the impact forces at different velocities. The capability of vehicle's structure to protect its occupants during the impact or crash is referring to the crashworthiness of a vehicle

Vehicle impact tests are conducted between 2 vehicles or between a vehicle and an obstacle (Cofaru, 2015). There are many standard crash tests and these standards are contained in Federal Motor Vehicle Safety Standards (FMVSS). For example, there are FMVSS 208 for frontal impact test, FMVSS 214 for side impact test and FMVSS 216 for roof crush test. Besides physical crash tests, computer simulation (Finite Element Model) have been widely used nowadays because it is precise and low cost.

2.4 Crash Test Program

In globally, numerous of safety assessment programs that perform crash tests has been established from time to time with the objective to improve vehicle safety and to supervise all vehicles manufactured have a good safety rating. The focus of these programs is to improve the crashworthiness of vehicles and lessen the number of injuries and fatalities. In Europe, there is the New Car Assessment Program (NCAP), introduced in 1979 by the

National Highway Traffic Safety Administration (NHTSA) in USA. In Australia and New Zeeland there is ANCAP, in Latin America there is LATIN NCAP, in China there is C-NCAP and in Germany, ADAC (Cofaru, 2015). ASEAN NCAP is the fourth NCAP in Asia continent after Japan, South Korea, and China (Jawi, Kassim and Sadullah, 2013). Figure 2.2 summarize all the NCAP programs in the world.

Continent	Country/Region	Program Name	Year Established
Asia	China	C-NCAP	2006
	Japan	J-NCAP	1991
	Korea	K-NCAP	1999
	ASEAN	ASEAN NCAP	2011
Australia	Australia & New Zealand	ANCAP	1992
Europe	France, Germany, Italy, Spain, Sweden, The Netherlands & UK	Euro-NCAP	1997
North America	USA (Insurance)	IIHS[a] Vehicle Ratings	1959
	USA (NHTSA[b])	US NCAP	1978
South America	Latin America & Caribbean	Latin NCAP	2010

[a]Insurance Institute for Highway Safety

[b]National Highway Traffic Safety Administration

Figure 2.2: NCAP PROGRAMS IN THE WORLD (Jawi, Kassim and Sadullah, 2013)

However, all programs across the globe use the same crash test protocols (Cofaru, 2015). Below is some common crash test protocol among the NCAP across the globe:

A. Full frontal impact test

B. Moderate overlap frontal test (formerly known as frontal offset test)

C. Small overlap frontal test

D. Side impact test

E. Roof crush test

2.4.1 Full Frontal Impact Test

A frontal crash is the most common type of crash resulting in fatalities. The frontal crash of a vehicle involves two collisions which the first collision occurs when the vehicle impacts with another vehicle or an obstacle such as a tree. Next, the collision between occupants in the vehicle with the compartment of the vehicle is known as the second collision ((NHTSA), 1989). Federal law (FMVSS 208 - occupant crash protection) make the requirement that all passenger cars must pass 30 mph in full frontal crash as compulsory. In the NCAP test, passenger vehicles are crashing into a rigid barrier at 35 mph that cover the full width of the vehicle. Some instruments are placed in the vehicle to record the response of the vehicle's structure during the crash. Anthropomorphic dummies are placed in the driver and passenger seats for the test, they measure the force of the impact to the chest, head and leg. Five-star rating assessment on vehicles are done by referring to these readings obtained from the impact test. In a nutshell, full frontal impact test program only involves with crashworthiness and acts as an indicator to tell how well a car can protect its occupants in a frontal collision (Ambati, Srikanth and Veeraraju, 2012). The configuration of full-frontal impact test is shown in Figure 2.3.

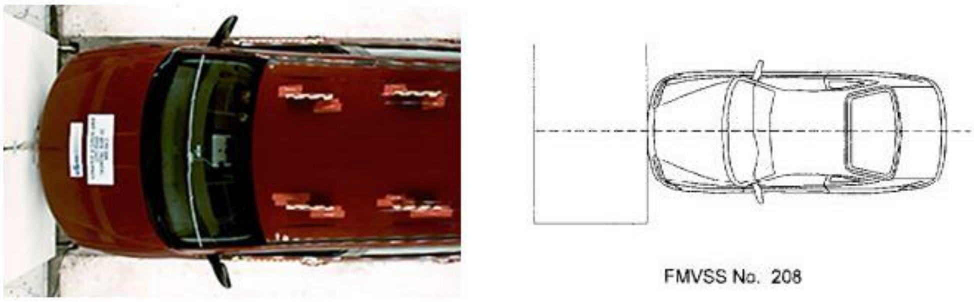

Figure 2.3: Full-width frontal test configuration (www.iihs.org/iihs/ratings/ratings-info/frontal-crash-tests)

2.4.2 Moderate Overlap Frontal Test (Formerly Known as Frontal Offset Test)

In the U.S., beginning in 1995, the Insurance Institute for Highway Safety (IIHS) introduced a program to give rating on safety of vehicles known as frontal offset test. This ongoing frontal offset testing program evaluates the crashworthiness of new model vehicles crashed into a deformable barrier made of aluminium honeycomb with over 2 feet tall. From experience of IIHS, they determined that a full-width test and a frontal offset test complement each other; a full-width test is especially demanding of restraints, while the offset test is demanding of the structural integrity of a vehicle (Park *et al.*, 1998).

In an offset crash, only one side of a vehicle's front end, not the full width, hits the barrier. Forty percent of the total width of the vehicle impacts the deformable obstacle on the driver side. The force in the test are similar to those that would result from a frontal offset crash between two vehicles of the same weight, each going just under 40 mph. As a result, a smaller part of the structure must manage the crash energy, and intrusion into the occupant compartment is more likely.

An offset test is more demanding of a vehicle's structure than a full-width test, while a full-width test is more demanding of safety belts and airbags. In a full-width test, there is less crushing of the vehicle structure so the decelerations that these restraints must handle are greater. By having both type of frontal tests, more complete picture of frontal crashworthiness can be captured than either test by itself (*Insurance Institute for Highway Safety, Highway Loss Data Institute*). The configuration of moderate overlap frontal test is shown in Figure 2.4.

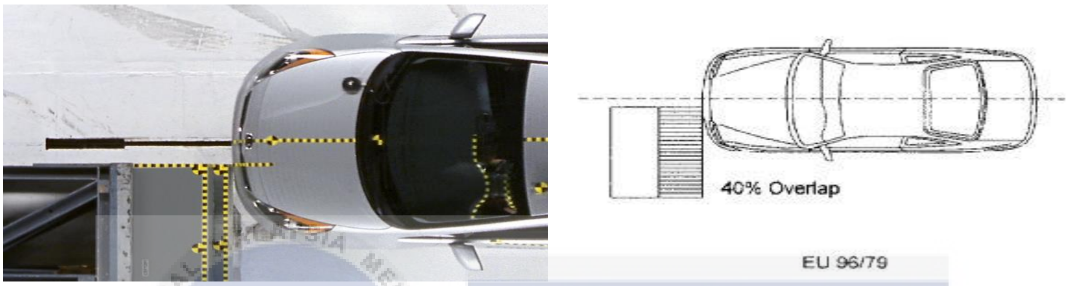

Figure 2.4: Moderate overlap frontal test configuration (www.iihs.org/iihs/ratings/ratings-info/frontal-crash-tests)

2.4.3 Small Overlap Frontal Test

In 2012, to inspire car manufacturers for further improvements in frontal crash protection, IIHS has developed a small overlap crashworthiness evaluation test (Sherwood *et al.*, 2013). The test is designed to replicate what happens when the front left corner of a vehicle collides with another vehicle or an object like a tree or utility pole. There are two types of small overlap frontal test, which are driver-side small overlap test and a passenger-side small overlap test (*Insurance Institute for Highway Safety, Highway Loss Data Institute*).

In the driver-side small overlap frontal test as shown in Figure 2.5, a vehicle travels at 40mph (64kmph) toward a 5-foot-tall rigid barrier and a vehicle overlap of 25 percent of its total width strike the barrier on the driver side. A Hybrid III dummy representing an average-size man is placed in the driver seat (*Insurance Institute for Highway Safety, Highway Loss Data Institute*).

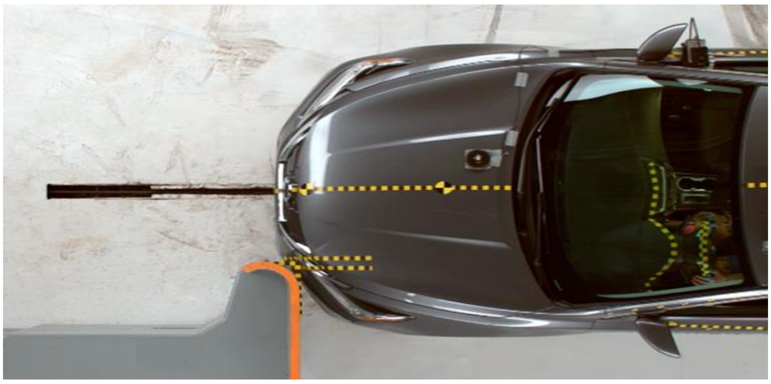

Figure 2.5: Driver-side small overlap frontal test configuration

(www.iihs.org/iihs/ratings/ratings-info/frontal-crash-tests)

Manufacturers have reacted to the driver-side small overlap test by improving vehicle structures and airbags, and most vehicles gain good ratings for this test at present. Despite, IIHS research tests discovered that those improvements didn't always applicable to the passenger side. Uneven improvements between the left and right sides of vehicles inspired them to develop a passenger-side small overlap test. In 2017, IIHS launched the ratings test for passenger side. The passenger-side test is similar to the driver-side test, difference is just that the vehicle overlaps the barrier on the right side instead of driver side as shown in Figure 2.6. Furthermore, the number of Hybrid III dummy involves increased to two instead of just one; one in the driver seat and one in the passenger seat (*Insurance Institute for Highway Safety, Highway Loss Data Institute*).

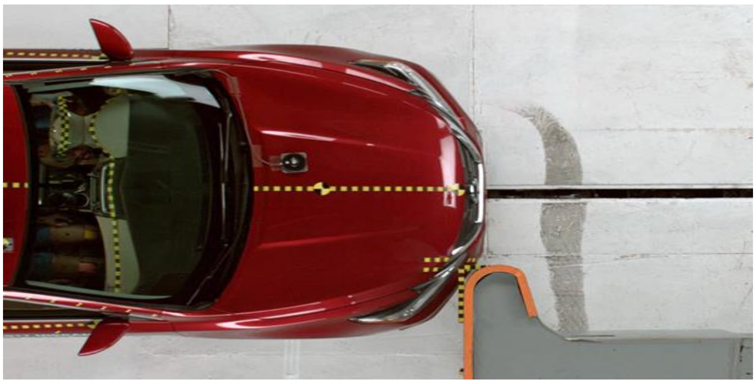

Figure 2.6: Passenger-side small overlap frontal test configuration

(www.iihs.org/iihs/ratings/ratings-info/frontal-crash-tests)

2.4.4 Side Impact Test

Rank just after frontal crashes, side impact crashes come second in the number of vehicle passenger deaths. Majority of the passenger vehicles have substantial crumble zones in the front and rear of the car, sides of vehicles have relatively little space to absorb energy (Reichert, R., Kan, Arnold-Keifer and Mueller, 2018). Side testing program has played a important part in bringing crucial improvements such as automakers have made big march for side protection by installing side airbags and strengthening vehicle's structure. Side airbags, which can be found on most new passenger vehicles today, are designed to constraint car occupants to colliding with the inside of the vehicle and with objects outside the vehicle in a side crash. They also help by spreading impact forces over a larger area of an occupant's body (*Insurance Institute for Highway Safety, Highway Loss Data Institute*).

Federal law (FMVSS 214 - side impact protection), a safety regulation issued by NHTSA in 1990. In 1997, NHTSA introduced a side impact crash tests consist of a stationary test vehicle impacts on the driver side by a crash cart fitted with a deformable barrier element. This side impact crash protocol is last modified in 2003. The latest test protocol is the 1,500 kg moving deformable barrier (MDB) has an impact velocity of 50 km/h (31.1 mph) and strikes the vehicle on the driver side at a 90-degree angle. Two SID-IIs dummies representing small (5th percentile) women or 12-year-old children are placed in the rear seat behind the driver and in the driver seat (Reichert, R., Kan, Arnold-Keifer and Mueller, 2018). The configuration of side impact test is shown in Figure 2.7.

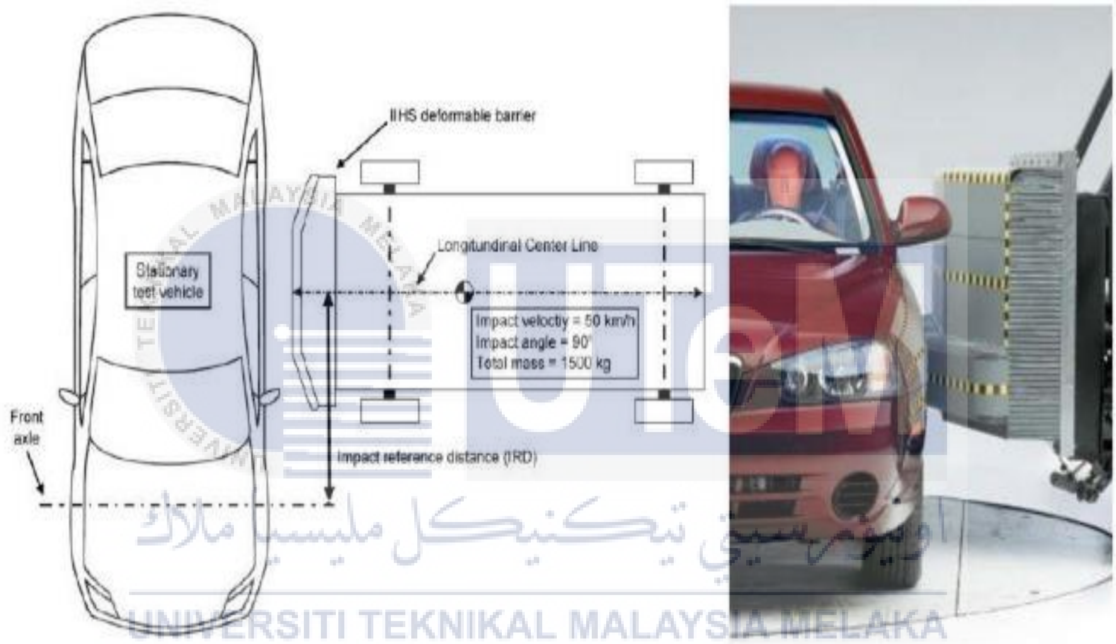

Figure 2.7: Side impact test configuration (Reichert, R., Kan, Arnold-Keifer and Mueller, 2018)

2.4.5 Roof Crush Test

Rollovers are crashes involving vehicle rotation of at least one-quarter turn (more than 90º) about a lateral or longitudinal axis. After rolling, the vehicle may come to rest on the side, upside down on the roof, or upright on all wheels (Conroy *et al.*, 2006). The main injured parts of occupants' body in rollover are the head and neck that contact with roof interior during rollover crash. The higher the intrusion in the roof structure during the rollover process, the greater risk of impact contact with occupant (Chen *et al.*, 2007).

The best approach to prevent these deaths is to prevent vehicles from rolling over in the beginning. Electronic stability control (ESC) is significantly lowering the risk of rollovers. When vehicles roll, side curtain airbags help to protect the occupants, and safety belt is also important. But, for these safety technologies to be most effective, the car roof needs to be capable to maintain the occupant survival space when it impacts with the ground during a rollover accident. With stronger roof, risk that people will be injured by contact with the roof itself will decreases because of less crushing. Stronger roofs also can stop occupants from being thrown out through broken windows, windshields or doors because the roof has deformed (*Insurance Institute for Highway Safety, Highway Loss Data Institute*).

Federal law (FMVSS 216- Roof crush resistance) introduced in 1973 specifies the strength requirements for passenger compartment roof of vehicles to protect occupants from injury due to roof intrusion during rollovers (Conroy *et al.*, 2006). Latest version of FMVSS 216 required the front corner of the roof to withstand a quasi-static force equal to at least 3 times the unloaded vehicle weight (UVW) of the light vehicles (gross mass under 2722kg or 6000 pounds). This is known as a strength-to-weight ratio (SWR) of 3.0 (Thakur and NATALE, 2009). In this test as shown in Figure 2.8, the force is applied by a flat test device at 25-degree roll angle (sideways) and 5-degree pitch angle (forward) in a downward direction on one side of the roof at a slow but constant speed and measuring the force required to crush the roof. The force applied relative to the vehicle's weight is the strength-to-weight ratio. The latest FMVSS 216 has implemented the two-sided test to replace the single-sided test (Thakur and NATALE, 2009). The key measurement of roof strength is the peak strength-to-weight ratio recorded before the roof is crushed 5 inches.

In the NCAP test, a good rating requires a strength-to-weight ratio of at least 4. This implies that the roof must withstand a force of at least 4 times the vehicle's weight before the plate crushes the roof by 5 inches. The minimum requirement is strength-to-weight ratio 3.25 to get an acceptable rating. Poor rating is given when the rating is less than 2.5 (*Insurance Institute for Highway Safety, Highway Loss Data Institute*).

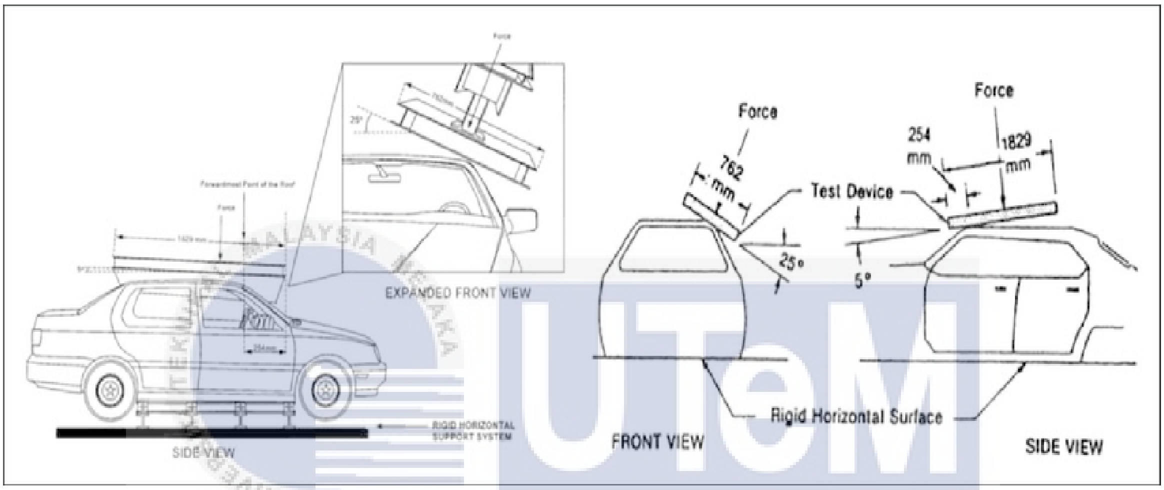

Figure 2.8: Roof crush test configuration (www.researchgate.net)

2.5 Underride Crash

According to the Fatality Analysis Reporting System (FARS), fatalities occur in crashes involving large truck is about 10 percent (Breu, Guggenbichler and Wollmann, 2008). Underride crashes happen when the front end of a vehicle impacts the rear or side of a larger vehicle, and slides under it. Underride may occur to some extent in collisions in which a small passenger vehicle crashes into the rear end or side of a large vehicles such as trailers because the bed and chassis of the impacted vehicle is higher than the hood/bonnet of the passenger vehicle. Accident data and case evaluations show that the majority of truck underrides occur in the 30mph (48kmph) to 50 mph (80kmph) range in term of relative velocity (Bloch *et al.*, no date).

In some severe underride crashes, the passenger vehicle underrides so far until the rear end or side of the trailer crushes the striking vehicle's A-pillars, windshield and/or roof area before the trailer strikes into passenger compartment of passenger vehicle. This condition is known as "passenger compartment intrusion" (PCI). PCI can result in severe injuries and fatalities to occupants. However, excessive underride can be hindered if an underride guard is installed on the larger vehicles. This prohibit PCI when it impacts the the smaller vehicle and prevent the vehicle from slide too far beneath the larger vehicle (NHTSA, 2015b).

The National Highway Traffic Safety Administration (NHTSA) published FMVSS No. 223 (Rear impact guards) and 224 (Rear impact protection) in 1996 and became effective in 1998. FMVSS No. 223 specifies dimensional, strength, and energy absorption requirements that rear impact guards must reach before installed on new trailers and semitrailers. FMVSS No. 224 requires that most new trailers and semitrailers with a GVWR of 4,536 kilograms (10,000 pounds) or more be equipped with a rear impact guard meeting FMVSS No. 223 specifications and specifies the location of the guard relative to the rear end of the trailer. These standards are expected to reduce injuries and fatalities resulting from the collision of light vehicles into the rear ends of heavy trailers and semitrailers (NHTSA, 2015a). Figure 2.9 below shows the research program by IIHS to develop a better underride guards by impacting a passenger car into a semitrailer with underride guard to check its effectiveness.

Figure 2.9: An IIHS research program to develop better underride guards

(https://www.iihs.org/iihs/sr/statusreport/article/49/7/1)

From the current worldwide efforts to reduce the number of injuries and fatalities in underride collison, it can be seem that almost all the safety measures are focused on the bigger colliding vehicle such as trucks and trailers. The federal laws required all trucks and trailers to be equipped with energy absobing rear, side and front underride guards. However, there is no mentioned about the safety measure to be focused on the smaller colliding vehicle in term of crashworthiness. Since the intrusion is usually involved the car roof's A-pillar before impact with the passengers in car, roof strength in A-pillar area of the smaller vehicle is an area worth to pay attention. Roof strength test should not only conduct based on the scenario of a rollover crash but also in an underride crash.

2.6 Impact Energy Absorption

Usually, there are two stages in car impact which are primary and secondary impacts. During the primary impact, which is collision between vehicle structure and rigid barrier, the large portion of crash energy is absorbed in the form of structural deformation that generates a crash pulse transmitted to the occupant compartment. Therefore, the scale of vehicle deformation will significantly affect the extent of passenger compartment intrusion (PCI). The vehicle deformation is depending on the vehicle design parameters such as strength of structural members, the vehicle mass, the available package space and the speed of impact. The impact between the interior vehicle compartment and the occupant is known as the secondary impact (Bois *et al.*, 2004). The impact energy delivered by the striking vehicle is calculated in terms of kilojoules, kJ using Eq. (2 1) (Hs, 2013).

$$E_{im} = \frac{\left(\frac{M_{im}}{2}\right) * V_{rv}^{2}}{1000} \quad (2.1)$$

Where E_{im} is Impact energy in kilojoules, M_{im} is Mass of striking vehicle in kilograms, V_{rv} is Relative velocity, in meters per second.

The Law of Conservation of Energy states that energy within a body or a system cannot be created or destroyed, and it may be transferred from one form into another, but the total energy will be remained the same. The parameter that causes injury is force, which can be measured with a force transducer (or load cell) or calculated from the acceleration of the body. The force acting on the passengers is governed by Newton's second law using Eq. (2.2):

$$\text{Force} = \text{Mass x} \frac{\Delta\, Velocity}{\Delta\, Time} \quad (2.2)$$

During the crash, the deformable structure of the vehicle will instantly absorb the force of crash by deforming and crumpling the areas affected by collision. The amount of deformation is equal to the stopping distance of the vehicle. Since the stopping distance of a vehicle in the crash is normally short and the stopping time is only a split second, a very high force is generated at the contact interface. A stronger structure absorbs more energy which enables more deformation to take place during a crash, therefore the stopping time will be longer and less forced transmitted to the car's occupant (Duane Bong).

The energy required to observe the collapse mode of material is defined as the energy absorbed. The measurement of energy absorption of a structure or system requires calculating the forces during the impact. The energy absorbed during an impact is given by the area under the graph of load versus displacement. The energy absorption is maximum if it is a rectangular profile for a given limits on force and displacement (Kamruzzaman, 2000).

2.6.1 Energy Absorption in Crash Involved Vehicle with Same Height

Crumple zone also known as crush zone, areas of vehicle that absorbs large portion of impact energy by deforming and crumpling during an impact. Front and rear of the car are usually the crumple zone and made of slightly lighter, more ductile materials than the rigid parts of the car passenger compartment as shown in Figure 2.10. For crash involving vehicles with same height or crash into a rigid body, with crumple zone, although the front section of the car immediately become stationary during a crash, it uses some time for the metal work to collapse because it is not a rigid body. This allows the middle and the rear of the section of the car continue to move for a short time. Since the stopping time is increased, the force acting on the occupant can be greatly reduced because less force is exerted to the rigid parts of the car (*Car Safety Features and Systems*, no date).

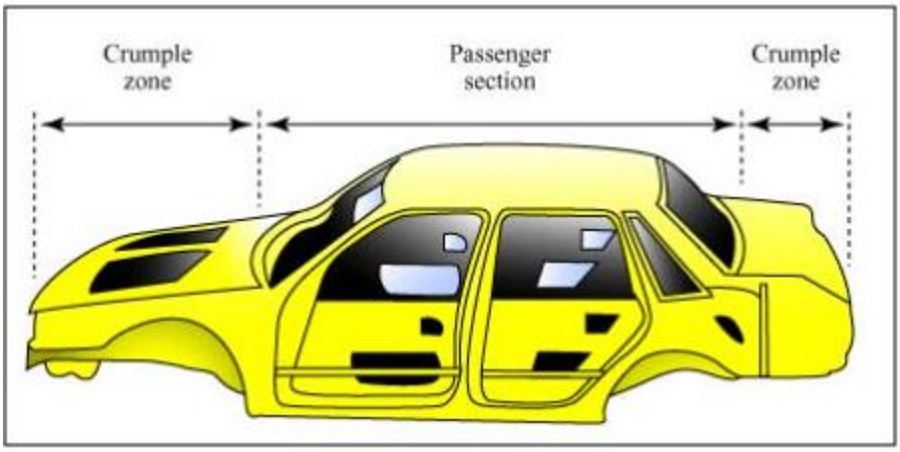

Figure 2.10: General crumple zones of a car (*Car Safety Features and Systems*, no date)

2.6.2 Energy Absorption in An Underride Crash

However, in underride crash, the biggest problem is the two impacting vehicles; large truck and small passenger vehicles are geometrically mismatch. The first point of the impact is between the truck and the A-pillar of the car along with the head of the smaller car's occupants because of the bottom of the truck is higher than the car hood. This condition bypasses the crumple zone of the car and no impact energy can be absorbed. As a result, underride always causes Passenger Compartment Intrusion (PCI) and hence cause severe injuries and fatalities.

While the structures deform and crumple, some of the energy generated during the crash is dissipated over a period of time. The energy to be dissipated by a car impacting a truck is given by Eq. (2.3) (Murray, 1988)

$$E = m_1 m_2 \frac{V^2}{2}(m_1 + m_2) \tag{2.3}$$

$$F = m_1 m_2 \frac{V^2}{2}(m_1 + m_2)s \tag{2.4}$$

Where E is the energy, F is the force acting between two vehicles, m_1 is car mass, m_2 is truck mass, V is car closing speed and s is crush distance.

The force, F is varying with truck mass as shown in Eq. (2.4). For a constant impact velocity, if the truck mass increased, force generated also greater. For a constant truck mass, increase impact velocity will also increase the force generated (Crashes *et al.*, 1991).

In underride crash, the energy is absorbed by rear, front or side underride guard that installed on the trucks and large vehicles. Today, the occupant crash protection features installed into vehicles are capable to provide high levels of occupant protection in 56 km/h (35 mph) frontal crashes. If guard is strong enough to remain in place and prevent PCI in crashes of severities of up to 56 km/h (35 mph), the impacting vehicle's occupant protection technologies could absorb enough of the crash forces resulting from the impact to significantly reduce the risk of fatality and serious injury to the occupants of the colliding vehicle (NHTSA, 2015b).

In addition, the purpose of this project is to study the crashworthiness of the roof pillars area including A pillar at the front, B pillar at the side, and C pillar at rear of the car which support the car roof. When the underride guard fails, these areas might be capable to aid the energy absorption and thus decrease the extent of intrusion into passenger compartment.

2.7 Finite Element Analysis (FEA)

The Finite Element Analysis (FEA) is a process to solve the governing differential equation of a mathematical model related to any physical condition using the numerical technique called Finite Element Method (FEM). The mathematical model can be static model or dynamical model depends on the actual physical situation. There are many FEA software available such as ANSYS, ABAQUS, NASTRAN, COSMOS. FEA is now used widely in automotive industry to conduct the crash and crash analyses. Linear static and dynamic analysis are conducted in routine manner in crash analysis (Kamruzzaman, 2000). Summary of a few researches using FEA simulation in automotive industry is presented in Table 2.1.

Table 2.1: Summary of some researches using FEA simulation in automotive industry

Researcher	Problem Studied	Result and Conclusion
(Abdel-Nasser, 2013)	Frontal crash simulation of vehicles against lighting columns	Current rigid lighting column absorbs little impact energy due to high yield strength, thus imposed high injury risk.
(Gohlami, Lescheticky and Paßmann, 2003)	ABAQUS/Explicit tested for crashworthiness simulation at BMW group.	ABAQUS/Explicit has been successfully tested and introduced into the productive crashworthiness simulation at BMW Group.
(Shenoy and Lankarani, 2006)	A study of energy absorption of a car roof reinforced with a grid stiffened composite panel in the event of a rollover.	Grid Stiffened Composite panels reduces the peak forces on the roof to an extent of 57% and increases the energy absorption by 80%. Thus, excellent choice for roof reinforcement involving impact situations.
(Bodapati, 2004)	Evaluation of energy absorption of newly designed underride guards for rear and side of large trucks.	The employment of new guards reduced the passenger compartment intrusions and reduced the underride of the car. With the new guards, the frontal crush zone of the car was fully utilized.

(Kumar *et al.*, 2018)	Crash Analysis of four wheels vehicle for different velocity.	Plastic deformation of the car increased with increase in velocity. Internal energy increased drastically and the kinetic energy decreased during the process of impact.

2.7.1 Abaqus

Abaqus is widely used in automotive and aerospace industry to carry out FEA. The Abaqus/Standard solver is to perform static analysis. For dynamic simulation, there are two methods available which are explicit and implicit procedure. For high speed dynamic events with relatively short dynamic response including general collisions, crash test, explosive events and bullet impacts, dynamic explicit solver is most suitable to use in Abaqus software. Abaqus/Explicit uses explicit time integration for time stepping (Kamruzzaman, 2000). To obtain a reliable result, time increments need to be small to prevent rapidly growing errors (Grimolizzi and Cravotta, 2015). For this project, dynamic explicit is selected because it is the most suitable method to investigate the case and time increment is set automatically by the software.

CHAPTER 3

METHODOLOGY

3.1 Project Planning

Before this project is started, all steps required to achieve the objectives are identified and planned. Firstly, the dimension of the existing car roof structure is measured and recorded. By using the dimension obtained, the 3D model of car roof structure is then modelled using CATIA software. Next, car roof 3D model is imported into ABAQUS software to perform Finite Element Analysis (FEA) and the impactor (lorry/truck) is created using ABAQUS software due to its simplicity. After that, the car roof model and impactor model are assembled by placing the rear end of impactor near to the A pillar of car roof structure to simulate frontal impact test on the car roof structure. Also, materials are created and assigned to each 3D model. A few essential parameters for the simulation such as step time, boundary conditions are identified and set before generating meshing for the assembly. By completing all steps above, the simulation is ready to run. After frontal impact test for car roof structure is done, the simulation is repeated for conducting side and rear impact test on the car roof structure. Finally, after all required simulations are completed successfully, results are analyzed and the final report is produced. The overall work is summarized in a flowchart in Figure 3.1.

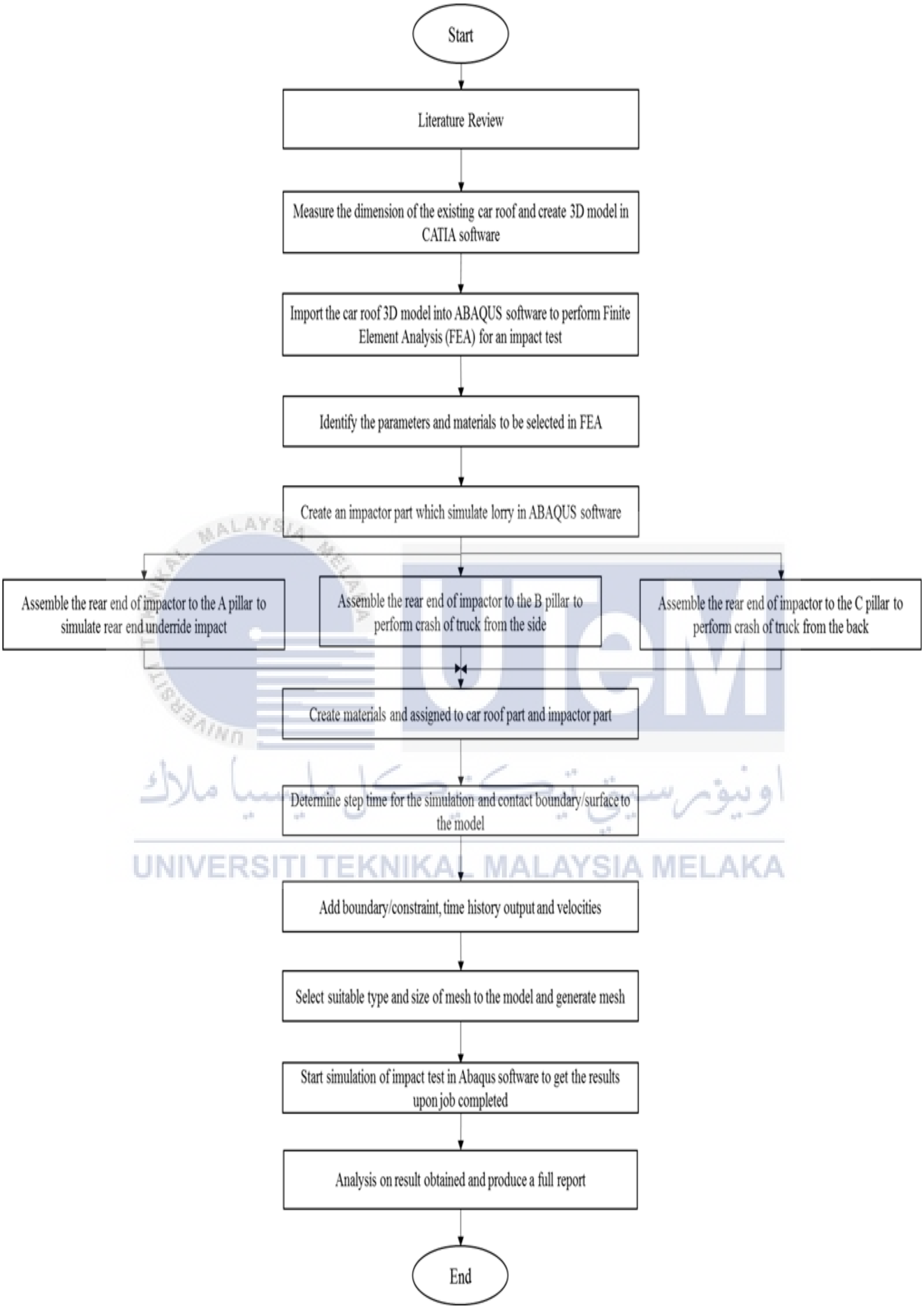

Figure 3.1: Flowchart of the project

3.2 Car Roof Selection and Measurement

The car roof model is taken from Proton Wira to study the energy absorbed at different sides of the car roof during an impact. Proton Wira is selected as the model for this project because it is readily available in Fasa B FKM and a 3D modelling was made by the previous batch of student, MUHAMMAD AFIFUDDIN BIN NOR AZLI, who studied the same project title. The car roof model developed by Afifuddin using CATIA software is focused on the car roof and its pillars only as shown in Figure 3.2. For this project, further development of the 3D model is required to improve the accuracy of the simulation result. The development includes fixing the small gaps found in the previously developed model because these gaps will cause error during meshing in FEA. Besides, the car roof model is further improved to simulate a much comprehensive car roof structure by adding neighbouring structure to it.

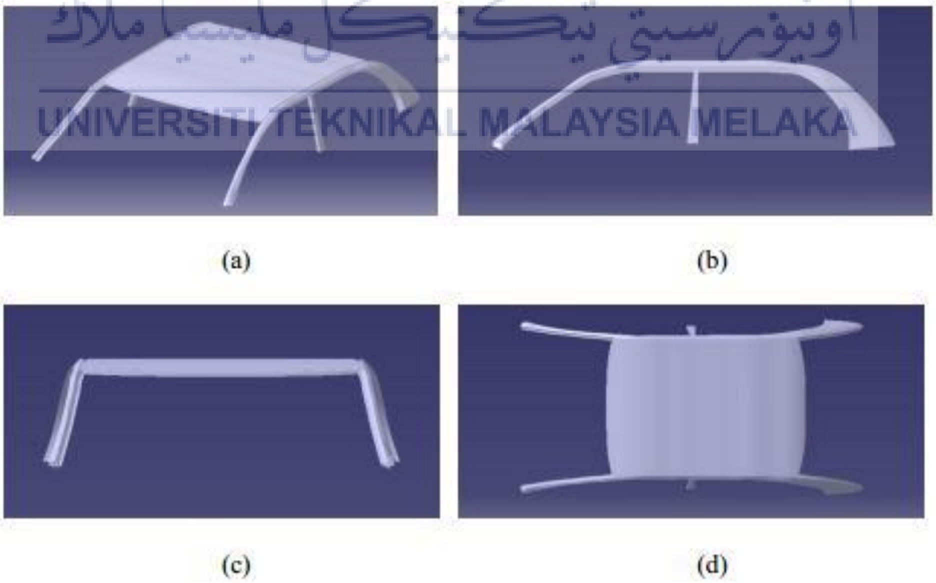

Figure 3.2: The car roof model developed by Afifuddin ;

(a) Isometric view, (b) Side view, (c) Front view, (d) Top view

(MUHAMMAD AFIFUDDIN, 2018)

To verify and improve the 3D model, point coordinate method is used to measure the dimensions of the actual car using measuring tape because the car roof is a complex geometry which consists of many curves. By measuring using point coordinate method, each point is measured of its location on X, Y and Z axis. A reference point (0,0,0) is set as the starting point to measure the location of other points. These points are marked on the adhesive tapes which stick on the car roof structure as shown in the figure below. Each of the adhesive tape is situated near to each other to capture a more accurate dimension. Figures 3.3 and 3.4 show how the points are marked and the method of measurement. Figure 3.5 show one of the areas where point coordinates are obtained to add neighbouring structure to the previous model.

Figure 3.3: The point coordinates and reference point

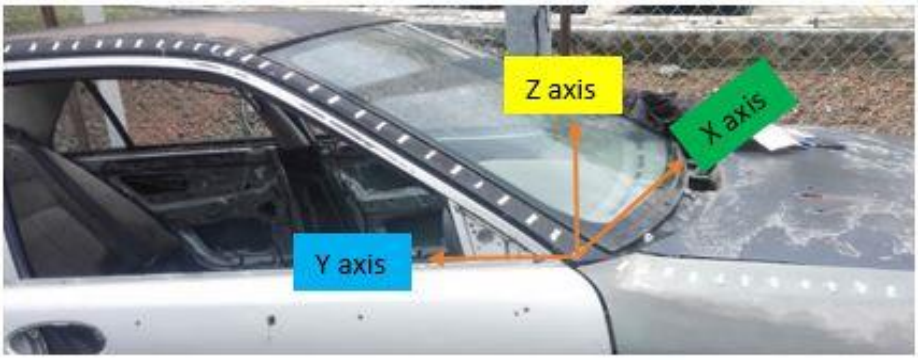

Figure 3.4: The X, Y and Z axis

Figure 3.5: Point coordinates to model the neighbouring structure of car roof

3.3 Car Roof Modelling

The 3D modelling is built using CATIA V5R19 software. The modelling process is started from zero by using point coordinates taken from previous developed model. Edit process is not done on the previous model file but rebuild the model from zero. This is because the commands in the previous model file are too many and edit by altering the commands might cause the children features linked to the specific command to fail and the whole model will eventually crash or fail. Hence, the model is repaired using previous point coordinates and improved the old model using current point coordinates to create the neighbouring structure of the car roof. The 3D modelling process is done on the wireframe and surface design workbench as shown in Figure 3.6.

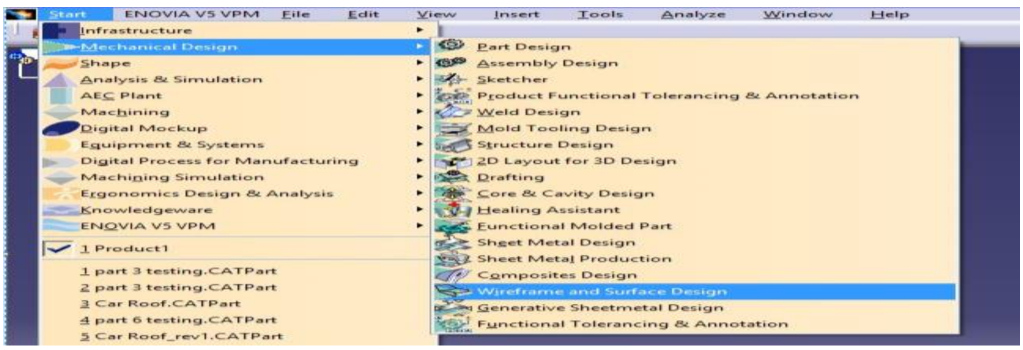

Figure 3.6: Wireframe and surface design workbench in CATIA V5R19

The first step of the modelling process is created a spline using points by inserting their coordinates as shown in Figure 3.7.

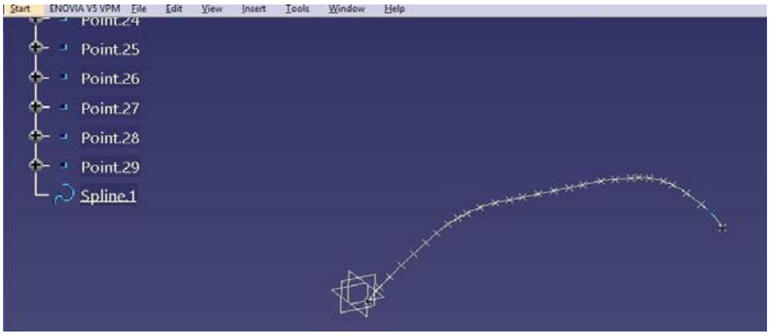

Figure 3.7: Step 1- spline is created using points

The second step is using the extrude surface feature to extrude the surface to half of width of the car roof from the spline created in step 1 as shown in Figure 3.8. It is extruded to half of the width of car roof only because the car roof is symmetrical in shape. Therefore, it only needs to model half of the car roof.

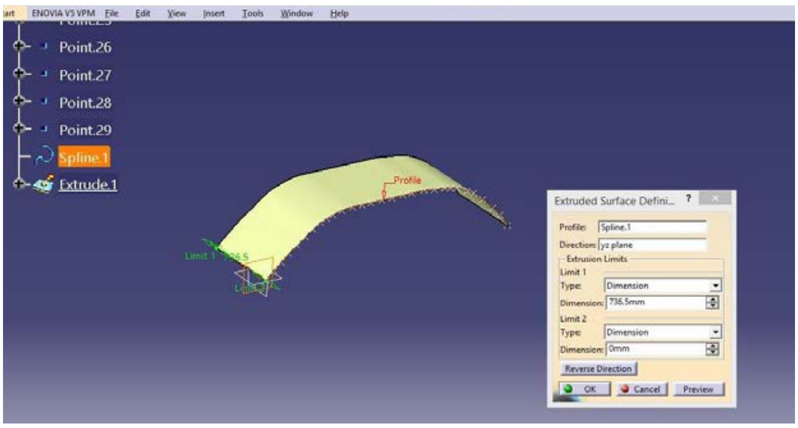

Figure 3.8: Step 2- extrude the surface to half of the width of the car roof

The third step is to create splines using points at front side of car roof and rear side of car roof and projected them onto the surface extruded from step 2. By using these splines, split surface feature is used to remove the frontal area and rear area of the roof top as shown in Figure 3.9.

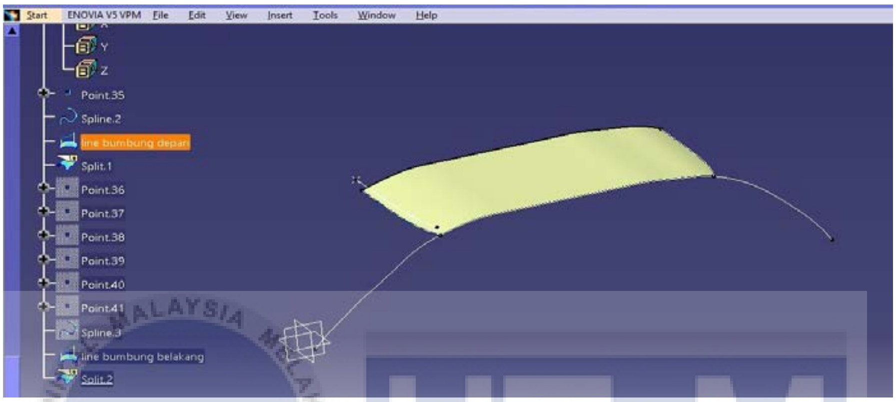

Figure 3.9: Step 3- split the unwanted surface on roof top

The fourth step is to create multiple splines to model the roof pillars as shown in Figure 3.10. The roof pillars are modelled because they are the support of the car roof which play important role in deciding the strength of car roof and hence will greatly influence the energy absorption property of the car roof.

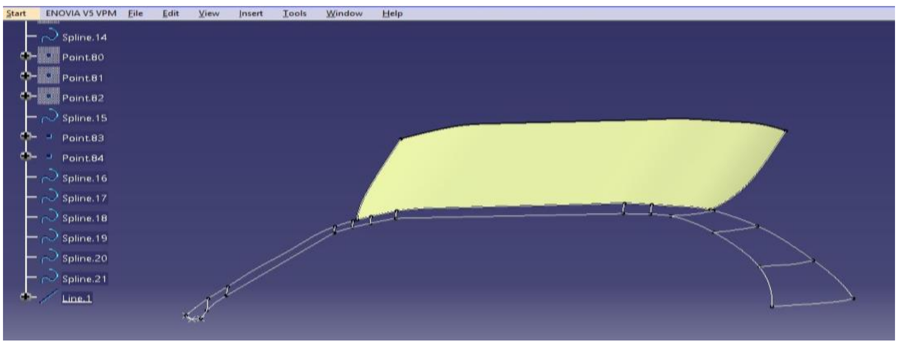

Figure 3.10: Step 4- Multiple spline to model pillars support

In Figure 3.11, it shown the fifth step which used fill surface feature to fill area connected by splines to create the surface of roof pillars.

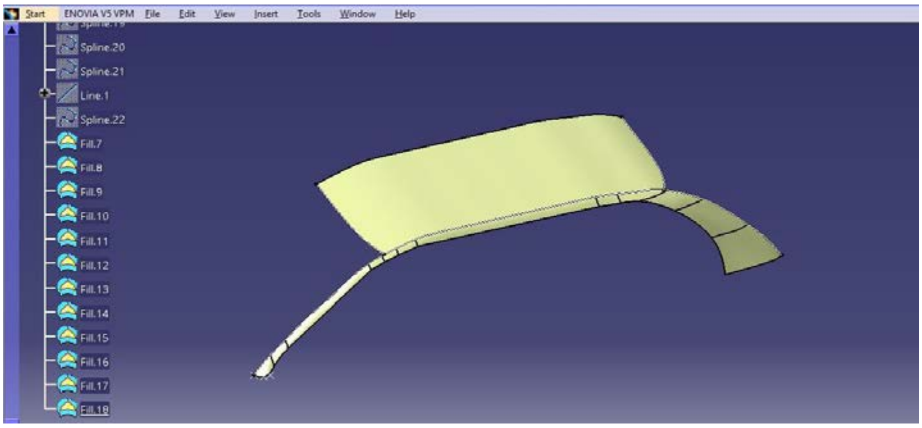

Figure 3.11: Step 5- Create surface of pillar supports

The sixth step is shown in Figure 3.12. A structure beneath the surface of car roof is created by sketched its profile and sweep it along the direction of car width. This structure is important because it enhances the strength of car roof and must not be neglected in this modelling process. In addition, the B pillar is also created using joined splines and fill the surface.

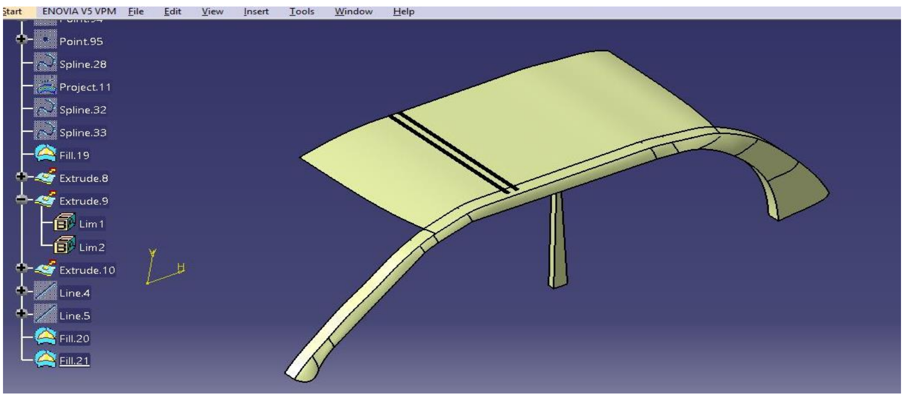

Figure 3.12: Step 6- Create B pillar and support structure beneath car roof surface

Figure 3.13 below shows two more support structure is created by using the symmetry feature. Planes are created in the middle in between the distance between two neighbouring support structure. By using symmetry feature, new support structure is created perfectly.

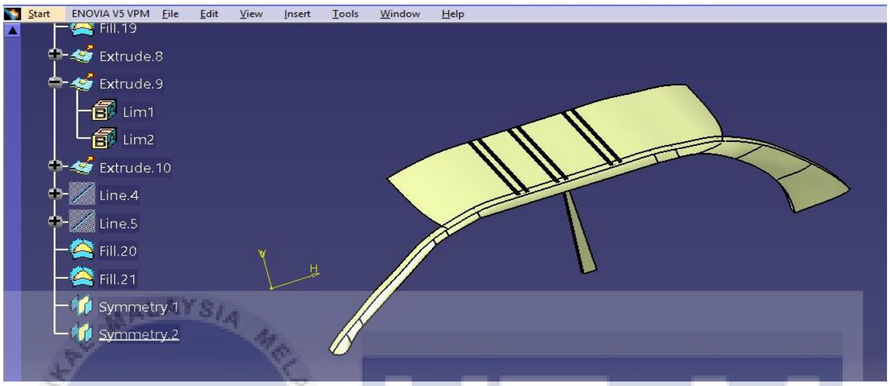

Figure 3.13: Step 7- Symmetry feature to create two more support structure

Figure 3.14 below shows the neighbouring structure added to the roof structure to improvise the overall model by using fill surface command. Then, use closed surface command to convert all surface to solid model by switching to part design workbench. Half of the 3D model is done after this step is completed.

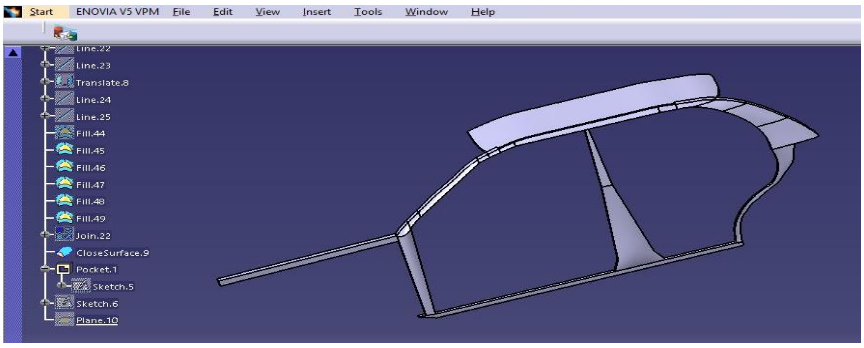

Figure 3.14: Step 8- Neighbouring structure is created

Lastly, the other half of the car roof model is mirrored command in the part design workbench. The completed 3D model is a solid car roof structure as shown in Figure 3.15.

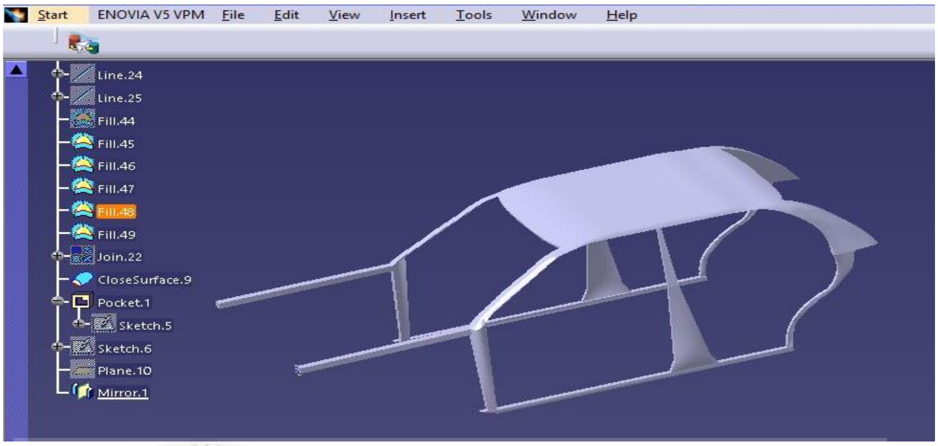

Figure 3.15: Completed 3D model of the car roof structure

Figure 3.16 shows the schematic drawing for the car roof. The drawing includes front view, top view, side view and the isometric view. The isometric view is set to a scale of 1:40. The dimension used is millimetre, mm.

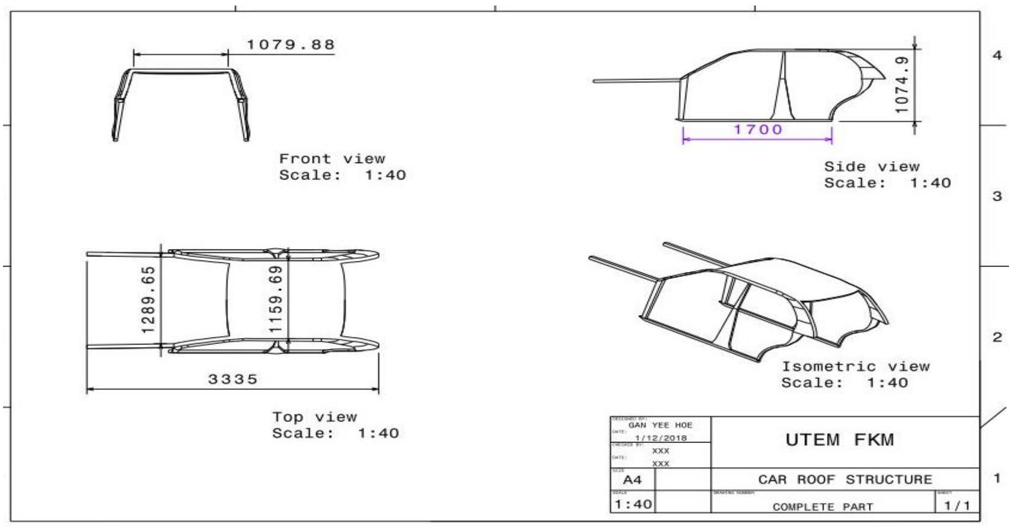

Figure 3.16: Schematic drawing of the car roof model

3.4 Parameters and Material Identification

After the 3D model is ready, the next stage of this project is to run the simulation of the impact test in ABAQUS software. However, the parameters and materials to be selected for the simulation need to be identified before initiating the simulation. Constant variables for this simulation are identified as the material of the impactor and car roof, velocity of the impactor and mass of the impactor. By referring to the protocol of the crash tests of trailers and their underride guards conducted by IIHS, the trailer model used for the test is 2015 Vanguard 53-foot dry van semi-trailer (IIHSA, 2016). The actual dimension of this trailer is shown in Figure 3.17. The properties of the trailer are listed in Table 3.1.

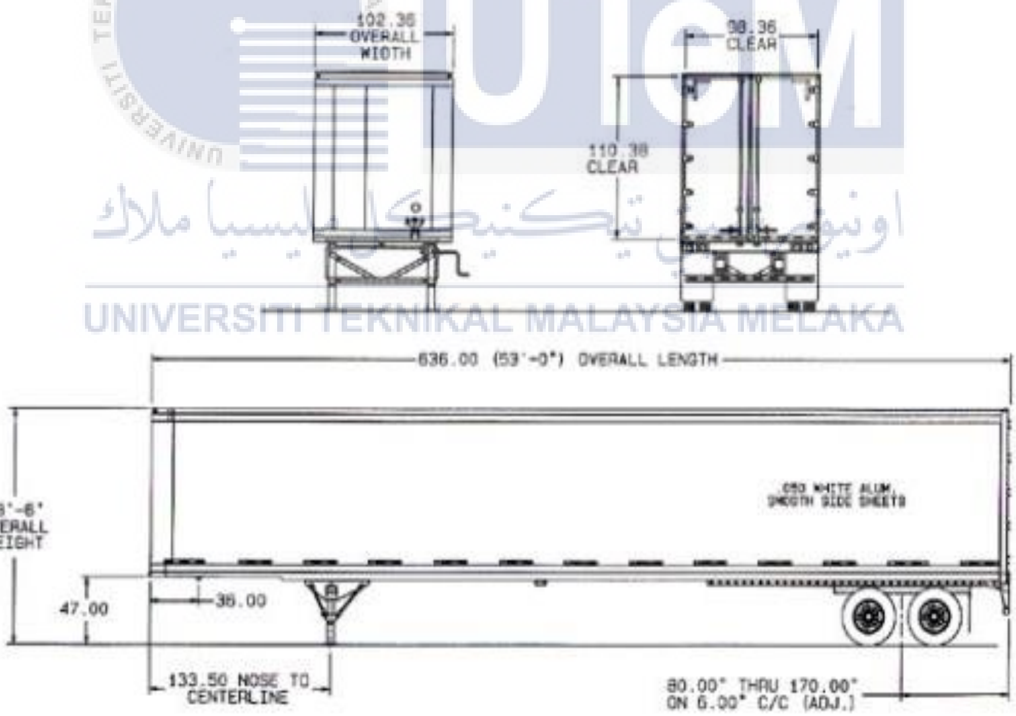

Figure 3.17: The dimensions of the 2015 Vanguard dry van semi-trailer (https://qbtransportation.com, 2018)

Table 3.1: Properties of impactor (IIHSA, 2016)

Properties of the impactor (trailer)	Value (units)
weight	6384 kg
Dimension (length × width × height)	16150 × 2591 × 2921mm
Height offset from ground	1190mm
Material	Galvanised steel

Next, the materials need to be assigned to the car roof structure and impactor is identified. The material selected for the car roof structure in this simulation is boron alloy steel, an ultrahigh-strength steel (UHSS). This is because roof rail reinforcement, roof pillars that support the roof is made of a type of boron alloy steel USIBOR 1500 (ArcelorMittal, 2010). For the impactor, the material selected is galvanised steel because trailers are mainly made from this material and more common to be found compared to aluminium due to its lower cost (https://www.heavydutydirect.ca/need-to-know-about-dry-van-trailers, 2018). The material properties to be used in the ABAQUS software for both impactor and car roof are listed in Table 3.2.

Table 3.2: Material properties for car roof structure and impactor (EFunda, no date)

Component	Material	Young's Modulus, E (GPa)	Density, ρ (kg/m3)	Poisson's ratio
Car roof structure	Boron alloy steel	190	7700	0.27
Impactor (truck)	Galvanised steel	200	7800	0.29

From past study, it revealed that when a passenger car travels at a speed of 70km/h and hits to a stationary heavy truck, the car will feel a deceleration of 35g or more which will translate to the passenger also. As the car speed increases from 70 to 100km/h, the impact increases directly to 46g which is possible of life threatening (Balta *et al.*, 2014). Considering also the speed limits in rural road in Malaysia is 90km/h as shown in Figure 3.18, and driver might slow down the vehicle before impact with the stationary truck is also an important factor (WHO, 2008). The reaction time is very short for the driver to response, so 80km/h is assumed as the impact velocity after the driver applied break to the car which travels at the 90km/h. After considering all these factors and the time constraint for this project, the impact velocities selected for this project are 80 km/h and 90km/h.

Table 3.2 Speed limits in urban and rural areas of selected lower and middle-income countries (not including motorways)

	Rural limit	Urban limit
Argentina	80–100 km/h	40–60 km/h
Kerala, India	70 km/h	40 km/h
Uttar Pradesh, India	No limit	No limit
Ghana	90 km/h	50 km/h
Indonesia	80–100 km/h	40–60 km/h
Malaysia	90 km/h	50 km/h

Figure 3.18: The speed limits in urban and rural areas in some countries including Malaysia (WHO, 2008).

3.5 Finite Element Analysis

In this study, ABAQUS software is used to conduct dynamic analysis for the impact test. After decided the model of trailer to be used as the impactor in the parameter and material identification stage, the impactor part will be created in the ABAQUS workspace. For this project, the impactor (trailer model) is simplified into a rigid mass. This rigid mass can be of any size since it represents only the mass of the vehicle (Grimolizzi and Cravotta, 2015). The weight of the trailer (impactor) is taken from the weight restriction order (Amendment) 2003 of Malaysia. According to this order, the lightest trailer is chosen with the maximum permissible weight of 16tonne as shown in Figure 3.19 (Yusak, 2018).

MAXIMUM PERMISSIBLE LADEN WEIGHT (BDM)
Rigid Vehicle - 2 Axles

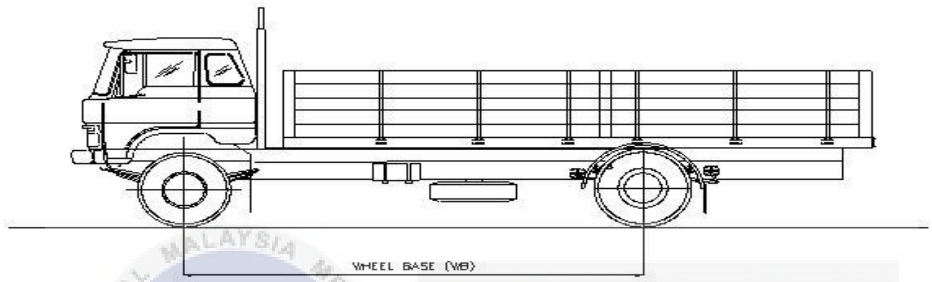

No.	Wheelbase (W/B)	Maximum BDM (Tonne)	
		List I (Peninsular)	*List II (Sabah & Sarawak)*
A.	< 2.3 M	16	14
B.	At least 2.3 M	17	15
C.	At least 2.6 M	18	16

Figure 3.19: The maximum permissible weight of a rigid vehicle with 2 axles in Malaysia (Yusak, 2018)

From the model of trailer used in IIHSA, 2015 Vanguard 53-foot dry van semi-trailer, the ratio of length, width and height of the trailer is determined and by referring the ratio, the dimension of the impactor to be used in the simulation is calculated to meet the targeted volume to represent the weight of 16000kg of the impactor. The finalised properties of the impactor model to be created is shown in Table 3.3.

Table 3.3: Dimension of impactor required for this analysis

Properties	Units
Density	7800kg/m3
Mass	16000kg
Volume computed	2.05m3
Dimension computed (length × width × height)	2256 × 1535 × 592mm

Before proceeding into ABAQUS software environment, it is important to identify which system of units to be used in the software because ABAQUS has no built-in system of units. All data input in this software must be specified in consistent units to prevent any potential of misinterpretation of the results obtained later. Some common systems of units are shown in Figure 3.20. For this project, system of SI (mm) is chosen.

Quantity	SI	SI (mm)	US Unit (ft)	US Unit (inch)
Length	m	mm	ft	in
Force	N	N	lbf	lbf
Mass	kg	tonne (10^3 kg)	slug	lbf s^2/in
Time	s	s	s	s
Stress	Pa (N/m^2)	MPa (N/mm^2)	lbf/ft^2	psi (lbf/in^2)
Energy	J	mJ (10^{-3} J)	ft lbf	in lbf
Density	kg/m^3	tonne/mm^3	slug/ft^3	lbf s^2/in^4

Figure 3.20: Consistent system of units in ABAQUS

3.5.1 Impactor Modelling

After dimension of the impactor is determined, the ABAQUS software is ready to use. The impactor created which has a weight of 16 tonne is shown in Figure 3.21.

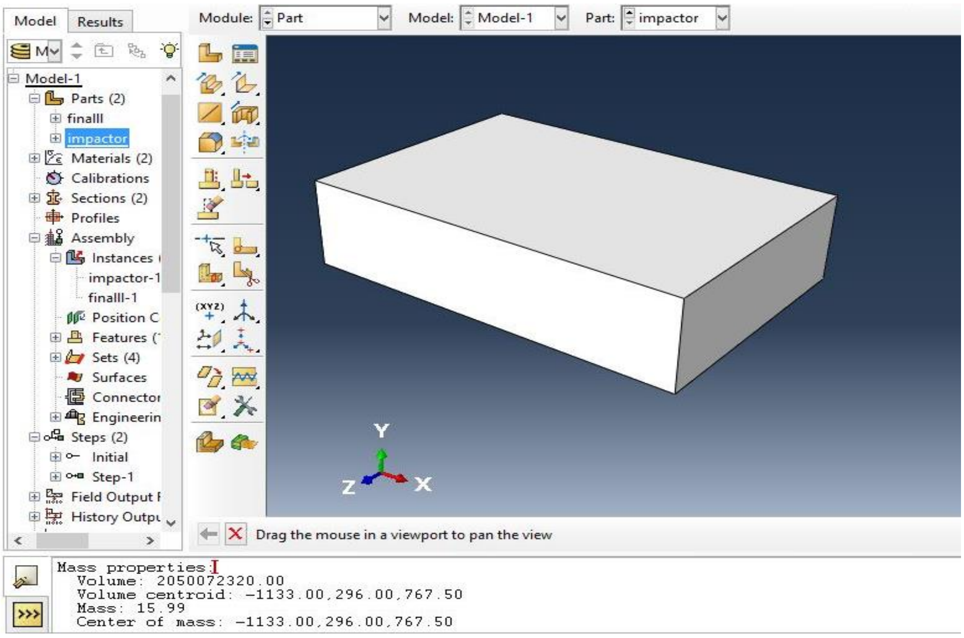

Figure 3.21: Impactor model created in Abaqus

3.5.2 Model Assembly

In this stage, the roof structure 3D model is imported into ABAQUS software to create a part. Now, there are two individual parts which is the roof structure and the impactor. To execute the simulation, individual parts need to be setup in such to simulate the real-world underride crash condition. To reduce the computation time and improve the efficiency of the simulation, the underride-guard the impactor is removed and the rear wall barrier of the impactor is moved to the front of the pillars of the car roof structure (Yang *et al.*, 2016). By using the “translate” and “rotate” command in the assembly module in ABAQUS, car roof structure and impactor are assembled as shown in Figure 3.22 for frontal impact test. These parts are not colliding with each other yet because in between there is a small gap provided during the setup. This is to make sure it is zero amplitude before the impact start because there is no any contact between these two individual parts in the beginning of the simulation (Ali *et al.*, 2011). The assembly is repeated for different orientation to simulate impact from side and rear of the car roof structure.

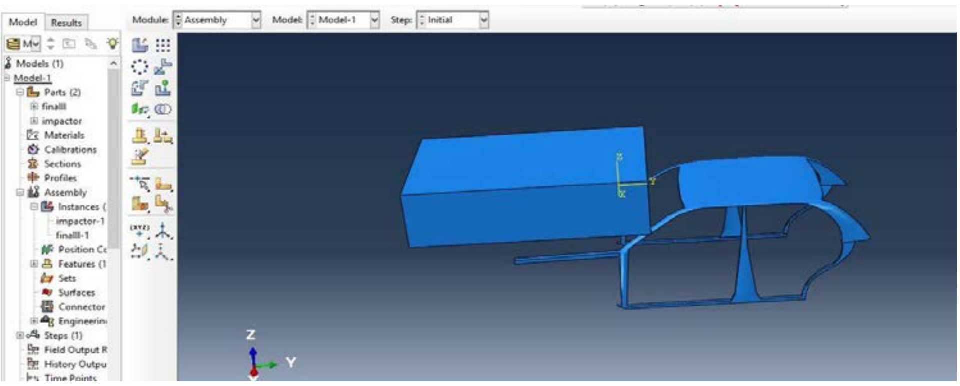

Figure 3.22: Assembled model for the frontal impact test

3.5.3 Material Properties and Assignment

In this stage, material properties are defined for car roof structure and impactor. The materials required are created and their behaviour such as density and elastic properties are inserted in the property module. The materials are then assigned to respective part. The materials created are boron alloy steel and galvanised steel which have been identified earlier in parameter and material selection stage. Figure 3.23 shown the density of the material being defined and its elastic properties are also defined as shown in Figure 3.24. Lastly, the materials created is assigned to respective part as shown in Figure 3.25.

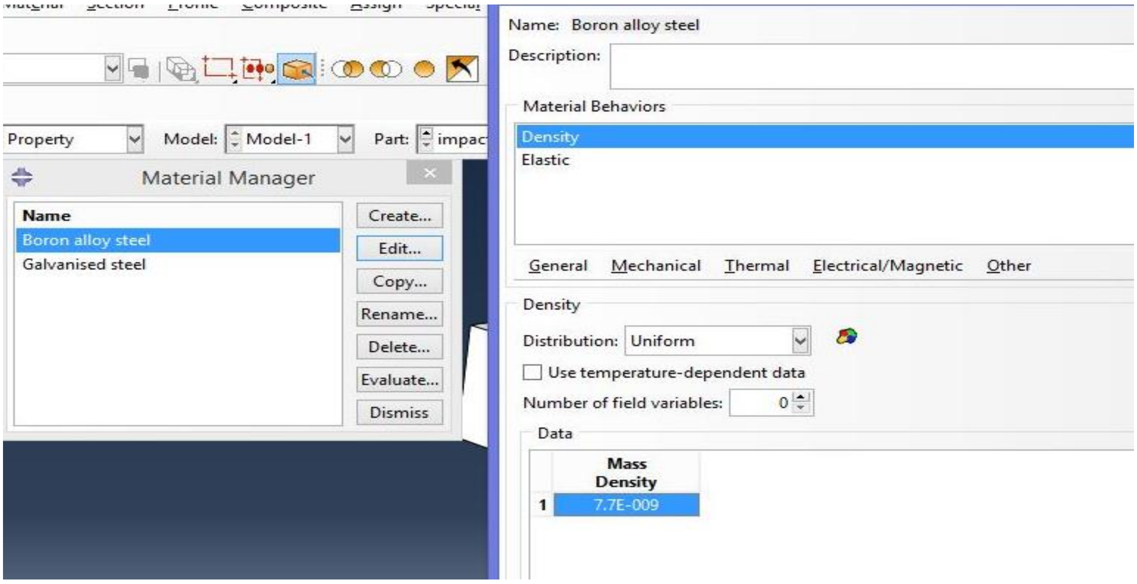

Figure 3.23: Define the density for the material

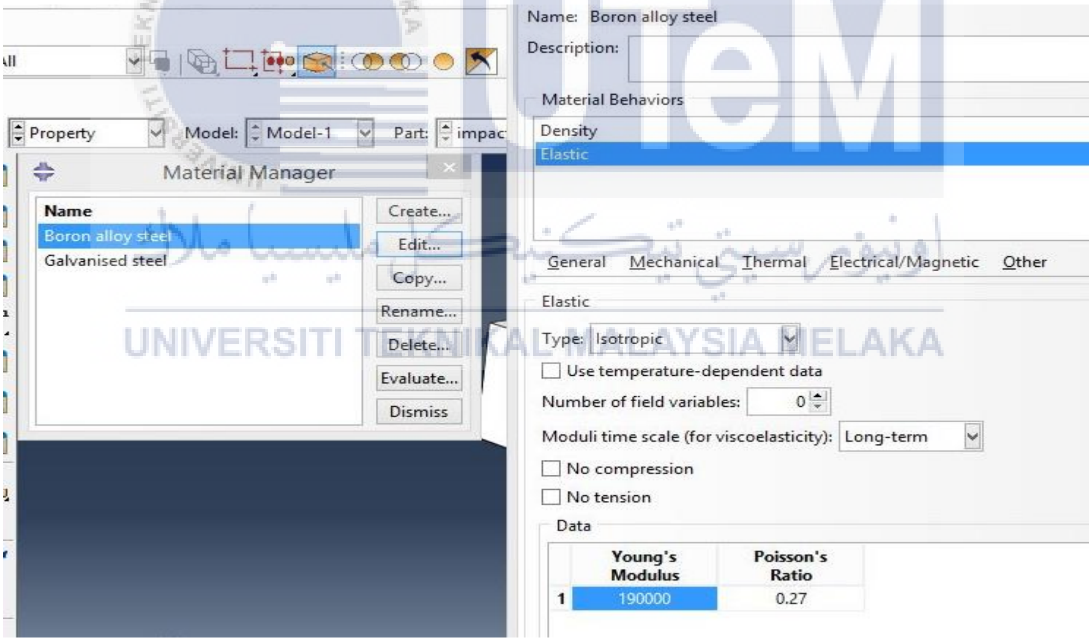

Figure 3.24: Define the Young's Modulus and Poisson's ratio for the material

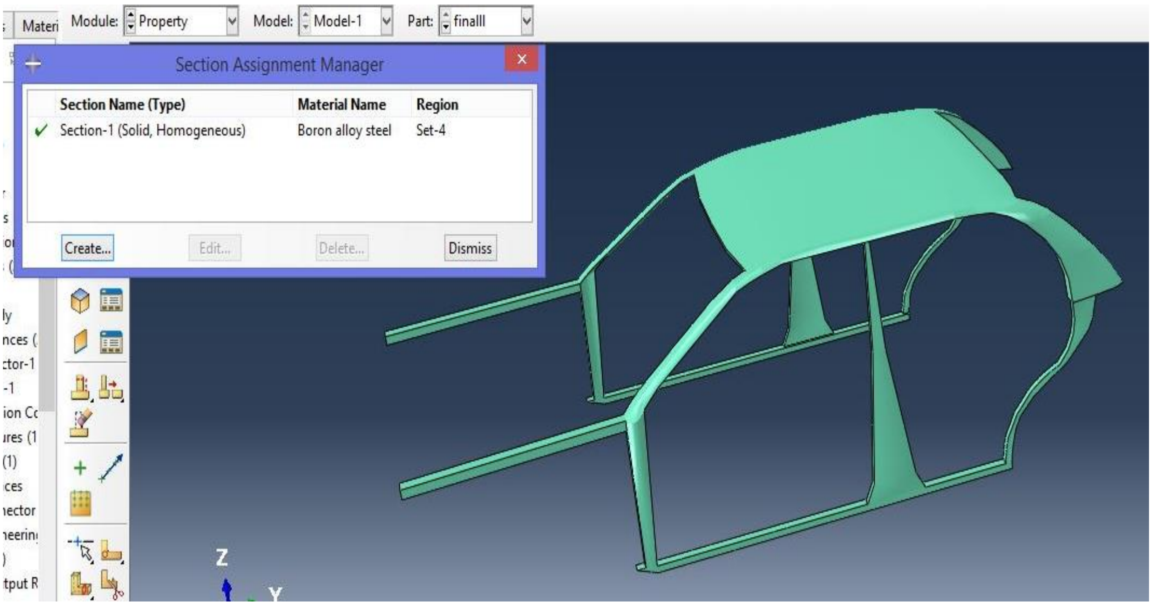

Figure 3.25: Assigned material to the part

3.5.4 Step Time

The next procedure in ABAQUS software is to set the step time for the simulation. Step time is the duration of the simulation step. By selecting the step module, Dynamic, Explicit is chosen for the step of this simulation and the time period is set to 0.02 seconds as shown in Figure 3.26. The step time 0.02s means that the impact simulation is occurs in just 0.02 second. By considering the time constraint, this step time is selected based on trial and error, a higher step time such as 0.1s will need a longer computation time.

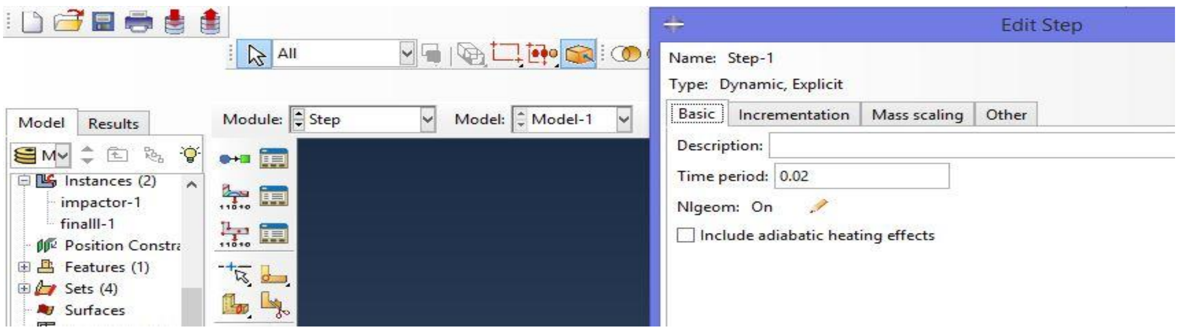

Figure 3.26: Define step time

3.5.5 Determine Contact Boundary/Surface to The Model

This stage is to define the contacts which come to interaction during the impact test. This is done by defining the interaction between the car roof structure and impactor by creating the interaction properties in the interaction module as shown in Figure 3.27. Next, for this impact test, dynamic explicit mode is chosen and general contact (explicit) interaction is created as shown in Figure 3.28.

Figure 3.27: Interaction properties created

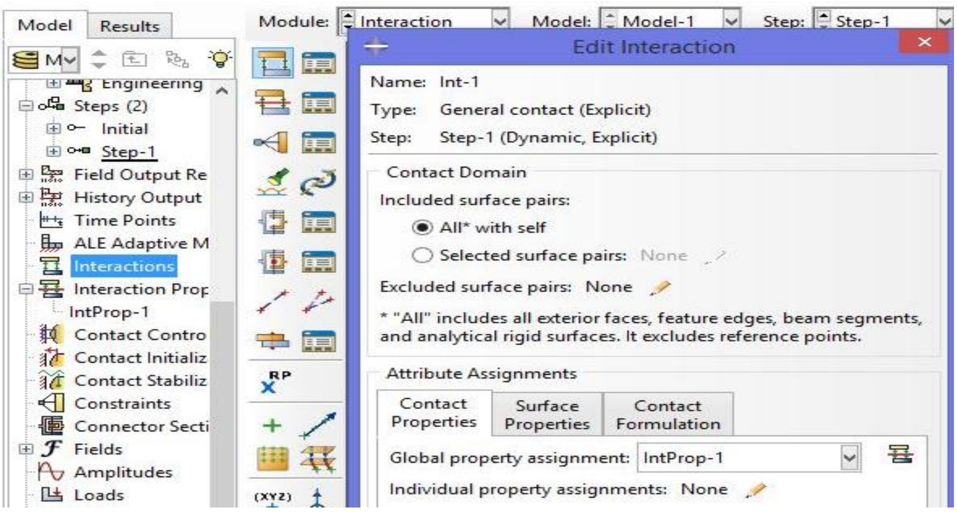

Figure 3.28: Interaction created

3.5.6 Apply Boundary Condition and Velocity to The Model

In this stage, boundary condition and velocity are created to simulate the car crash into the rear side of the impactor. As the tyres of the car are fixed to the ground during the impact, encastre (zero translation and zero rotation) type boundary condition is picked for the bottom structure of the car roof structure model to constraint the model in all degrees of freedom as shown in Figure 3.29 (Reddy, 2013). For the impactor, it is assigned to velocity type of boundary condition in the impact direction, which is towards the car roof structure as shown in Figure 3.30.

After the boundary conditions are all set for the assembly, the models are ready to be meshed. Figure 3.31 shows the overall boundary conditions for the frontal impact test assembly.

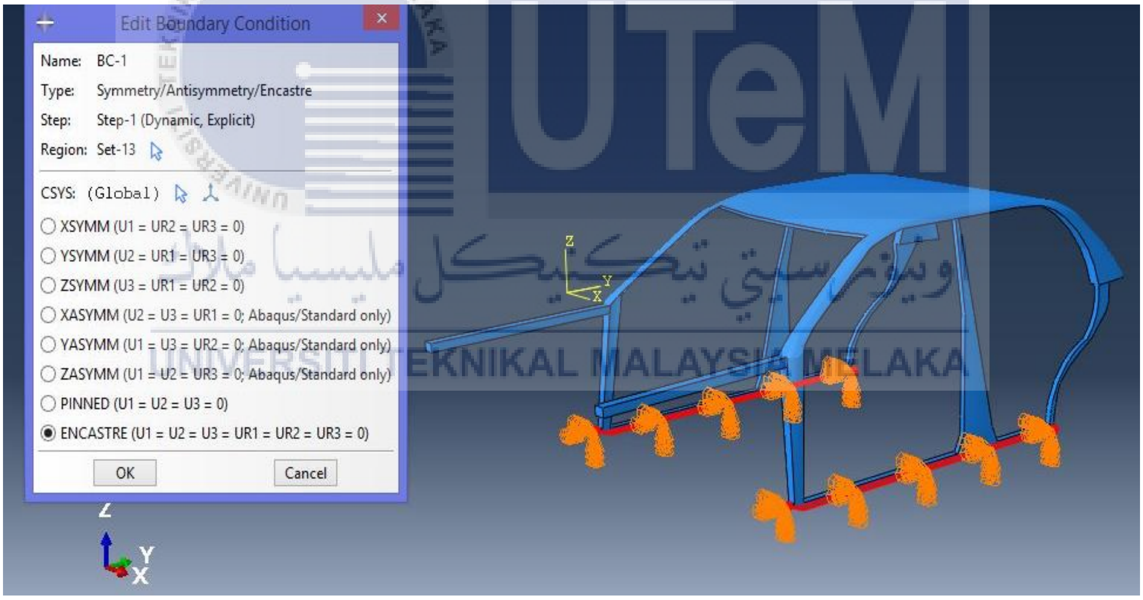

Figure 3.29: Boundary condition of car roof structure model

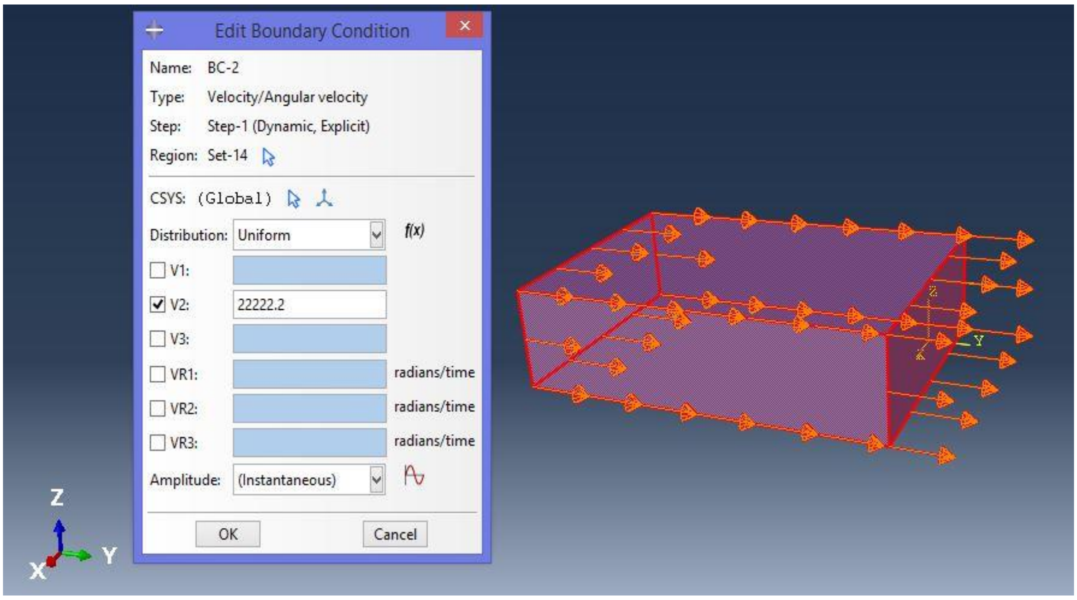

Figure 3.30: Boundary condition of impactor

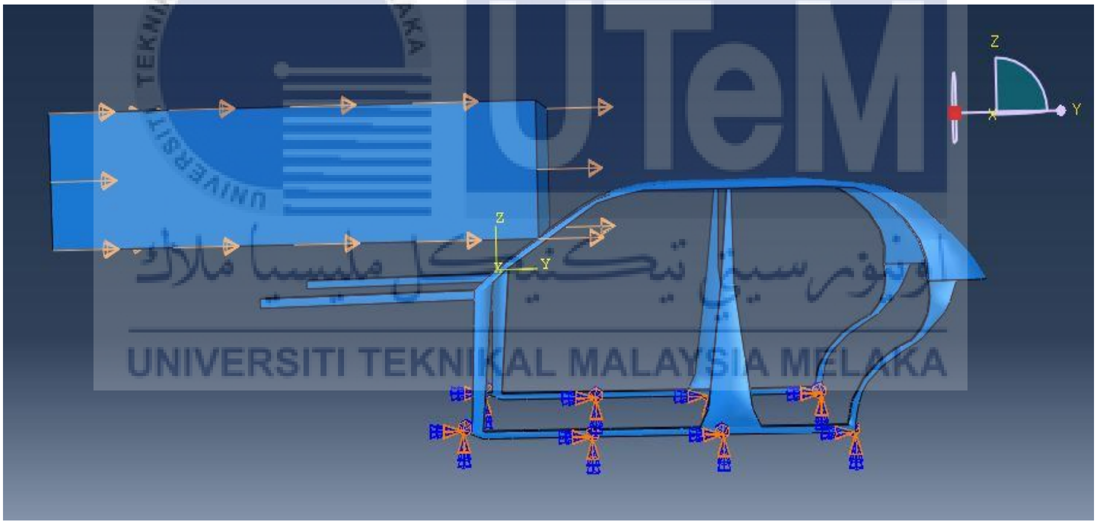

Figure 3.31: Boundary conditions for the frontal impact test assembly

3.5.7 Apply Mesh to The Model

Hexahedral-shaped element is chosen to mesh the impactor due to its simple geometry. For car roof structure, tetrahedral-shaped element is chosen to mesh the part due to the complexity of its geometry (Chang and Yang, 2009). Next, the mesh size is defined for each of the part separately. In general, a smaller meshing size provide a higher accuracy to the results obtained, but it will take a longer computation time. In this project, the global mesh size of the impactor is kept constant at 60mm throughout all the simulations involved as shown in Figure 3.32. However, global mesh size of the car roof structure is varying for each impact test; 85mm, 60mm, 40mm, 30mm and 20mm as shown in Figure 3.33. This difference in mesh model is to study the effect of mesh density to the result of test data from simulation (Liu and Glass, 2013). After the mesh generated, mesh data is tabulated in Table 3.4.

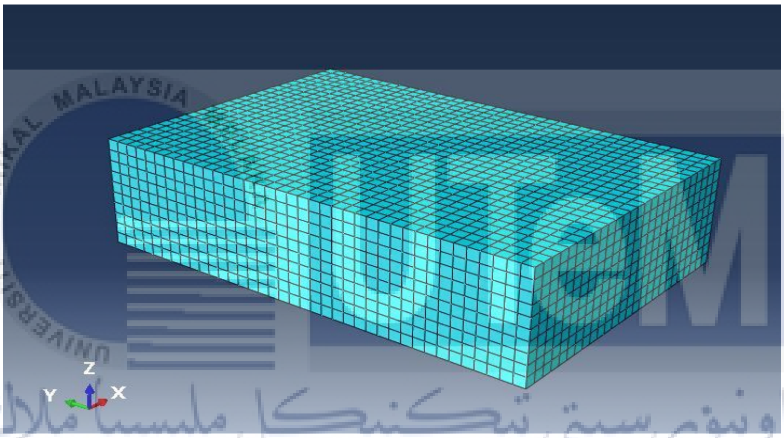

Figure 3.32: Impactor with constant mesh size of 60mm for all simulations in this project

Table 3.4: Mesh data for car roof structure with different mesh size

Mesh Size (mm)	Number of Elements	Number of nodes
85	4192	9260
60	7075	15268
40	13157	27696
30	23595	47913
20	63044	118254

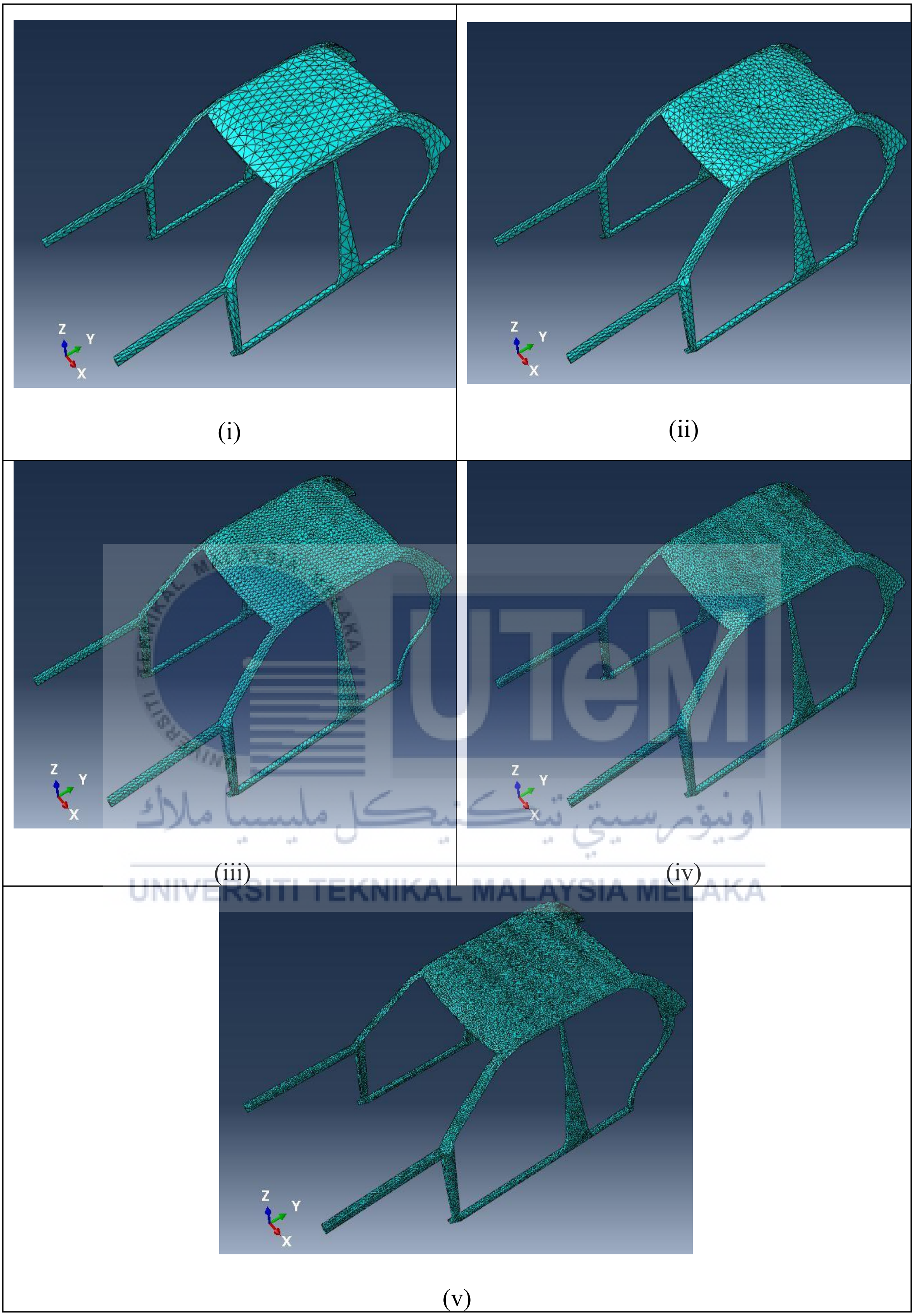

Figure 3.33: Car roof structure with different mesh size;

(i) 85mm, (ii) 60mm, (iii) 40mm, (iv) 30mm, (v) 20mm

CHAPTER 4

RESULT AND DISCUSSION

4.1 Introduction

This section explains on the result of the impact test using finite element analysis obtained from 3 different type of impact simulations which are simulation of frontal, side and rear impact test on the car roof structure. Each type of impact simulation involves with impact velocity of 80km/h (22222.22mm/s) and 90km.h (25000mm/s). For each type of impact, there are 10 simulations with each impact velocity conducted by using 5 different mesh sizes of the car roof structure; 85mm, 60mm, 40mm, 30mm and 20mm. Upon completion of simulations, the data of Reaction Force (N) and Displacement(m) are extracted from three nodes which located in the region where the impactor experienced the greatest reaction force during the impact to get the average reaction force to obtain a more precise result. The data is then used to plot the graph of Force (N) vs Displacement (m). After obtained the data, Origin Pro software is used to calculate the area under the curve of the graph which represents the energy absorbed by the car roof structure during the impact. The energy absorbed for each simulation is neatly presented and the discussion is then continued.

4.1.1 Data Collection Method

During the simulation, the reaction force is captured by the impactor and the results are extracted from the nodes with distinct reaction force value (Patil and Panchwadkar, 2014). The impactor is used to extract the data because its mesh size remains constant throughout all cases of simulation, this allow us to make comparison by having the different data obtained from the same nodes in every different simulation. For every single simulation analysis, three nodes ; node 43, node 142 and node 263 which are located in the area where the impactor in contact with the car roof structure during the impact are used to extract the data required. These nodes are located on the same horizontal line in the area where the impactor experienced the greatest reaction force as shown in Figure 4.1. In each case of different meshing size, the same nodes are used to extract the data of reaction force and displacement. This is to ensure that the analysis on energy absorbed can be done by comparing the result obtained from the same nodes for different meshing size and different type of impact test (front, rear or side).

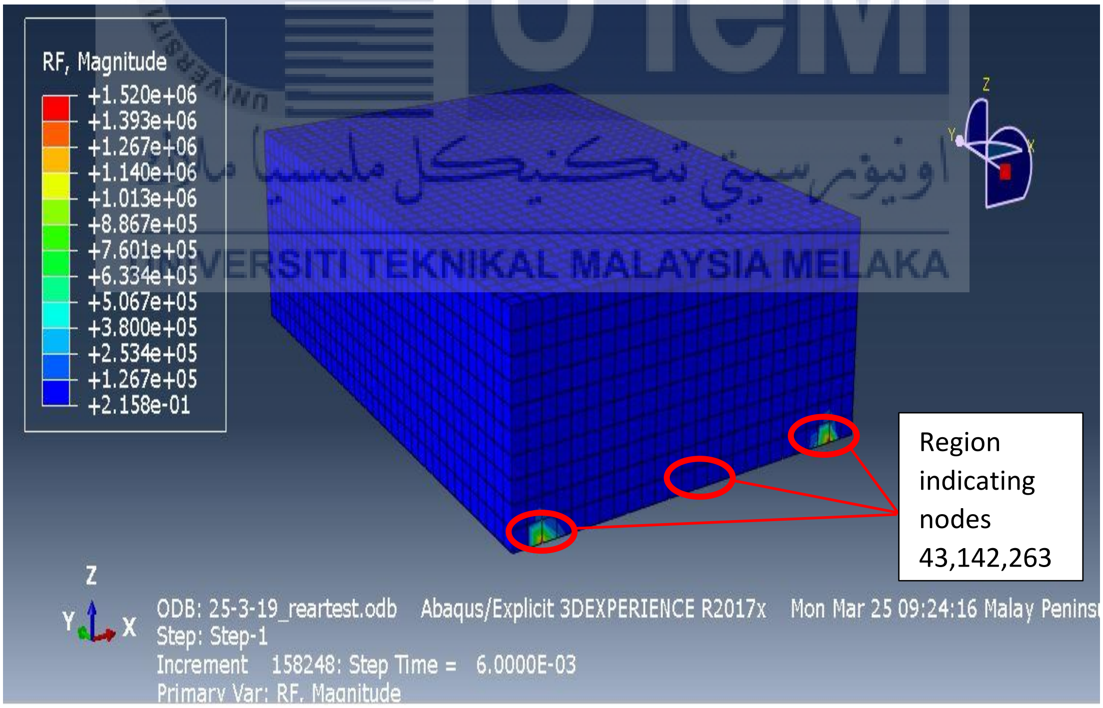

Figure 4.1: Nodes selected to extract data for determine energy absorbed

4.2 Frontal Impact Test Simulation

Figure 4.2 shows the model assembly setup before the frontal impact test simulation while Figure 4.3 shows deformed car roof structure after simulation. Since the bottom of car roof structure is fixed to the ground, the body deformed at the upper area of the frontal roof structure, especially A-pillars. The average displacement of impactor in time span of 0.02s are 0.44m and 0.50m for 80km/h and 90km/h respectively. The displacement and reaction force at the striker are collected from nodes selected. The graphs of reaction force versus displacement for 80km/h and 90km/h are shown in Figure 4.4 and Figure 4.5 respectively.

Figure 4.2: Undeformed car roof structure before frontal impact simulation

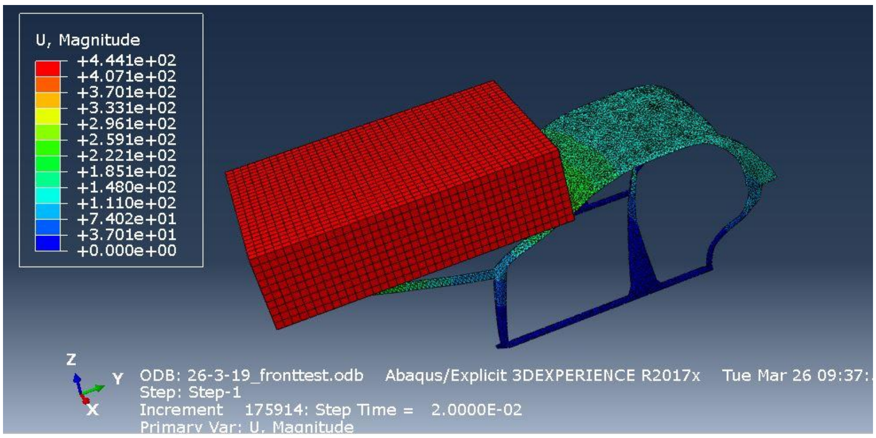

Figure 4.3: Deformed car roof structure after frontal impact simulation

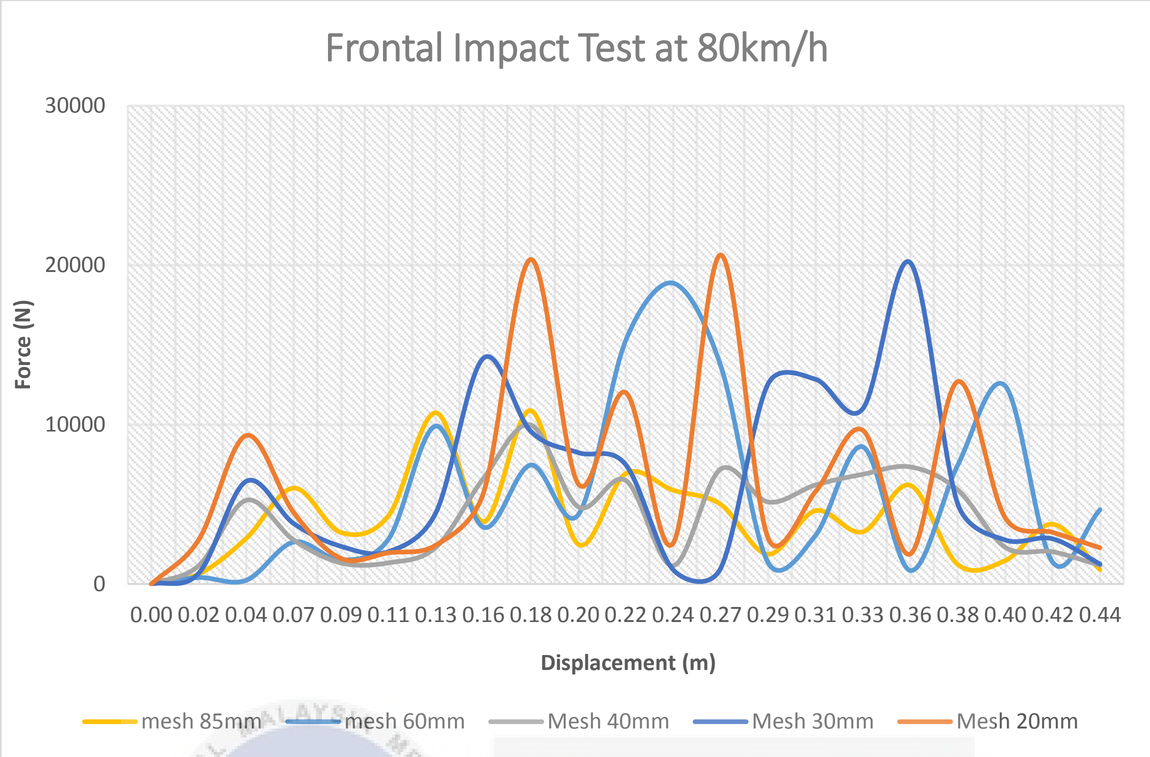

Figure 4.4: Force-displacement curves for frontal impact test with impact velocity of 80km/h

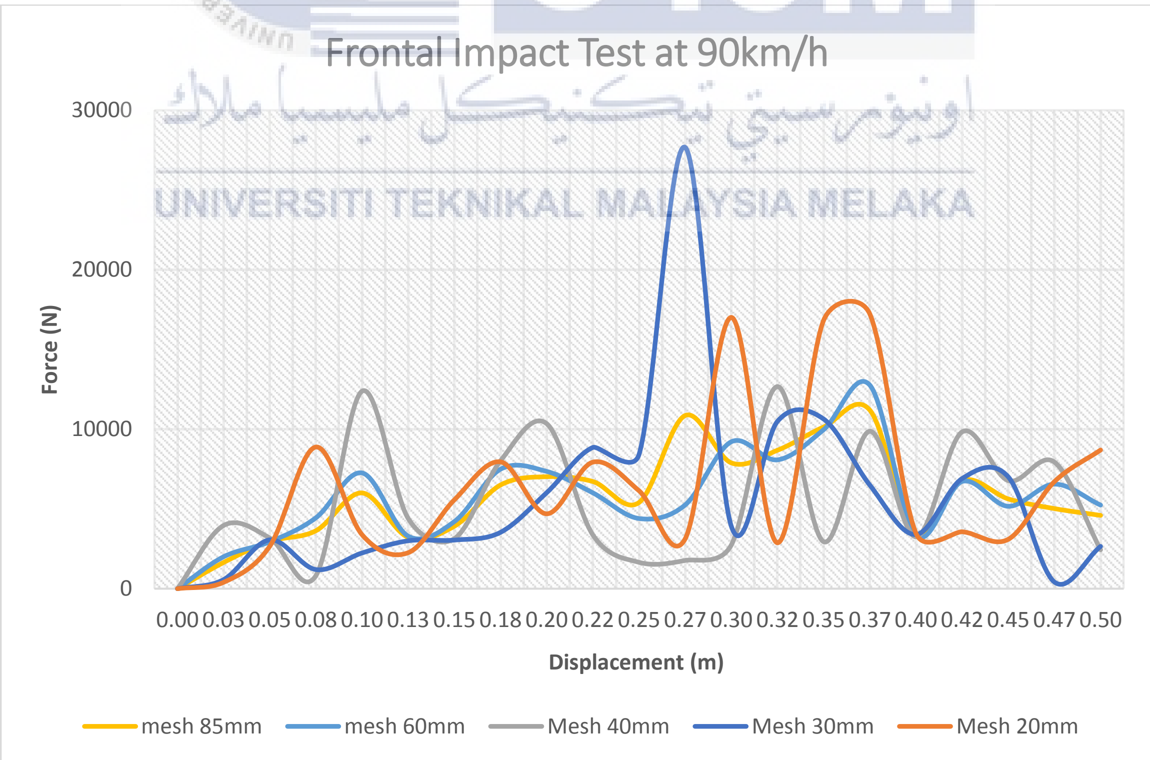

Figure 4.5: Force-displacement curves for frontal impact test with impact velocity of 90km/h

4.3 Side Impact Test Simulation

Figure 4.6 shows the model assembly before the side impact test simulation while Figure 4.7 shows deformed car roof structure after simulation. Since the bottom of car roof structure is fixed to the ground, the body deformed at the upper area of the side roof structure, especially B-pillar. The average displacement of impactor in time span of 0.02s are 0.44m and 0.50m for 80km/h and 90km/h respectively. The displacement and reaction force at the striker are collected from nodes selected. The graphs of reaction force versus displacement for 80km/h and 90km/h are plotted as shown in Figure 4.8 and Figure 4.9 respectively.

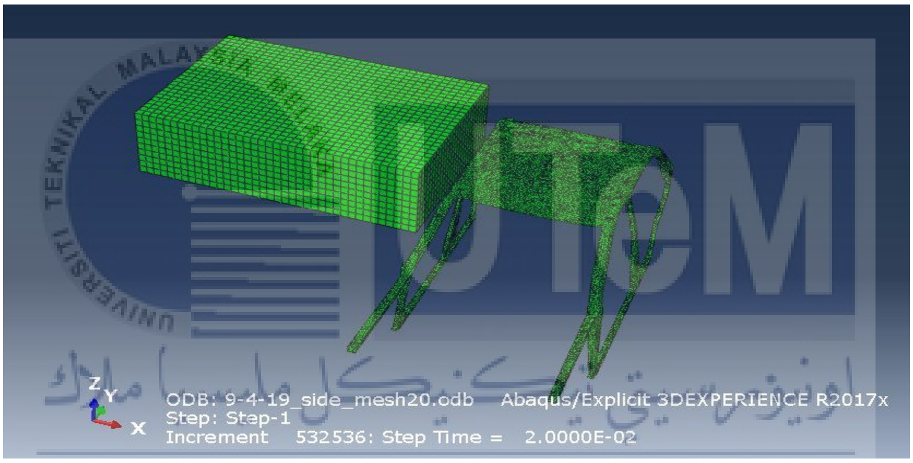

Figure 4.6 : Undeformed car roof structure before side impact simulation

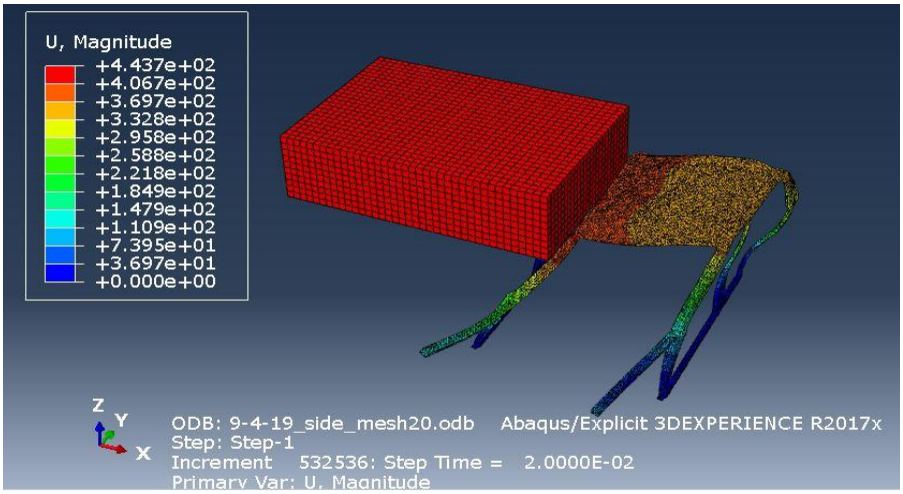

Figure 4.7 : Deformed car roof structure after frontal impact simulation

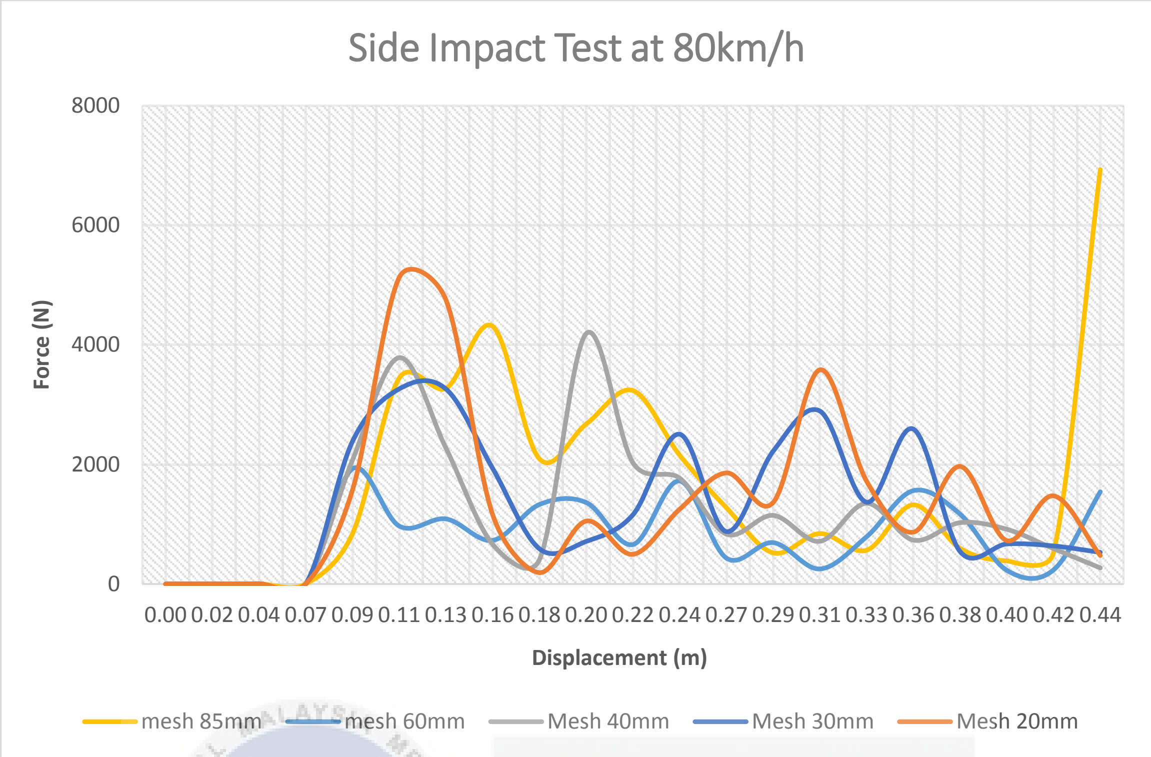

Figure 4.8: Force-displacement curves for side impact test with impact velocity of 80km/h

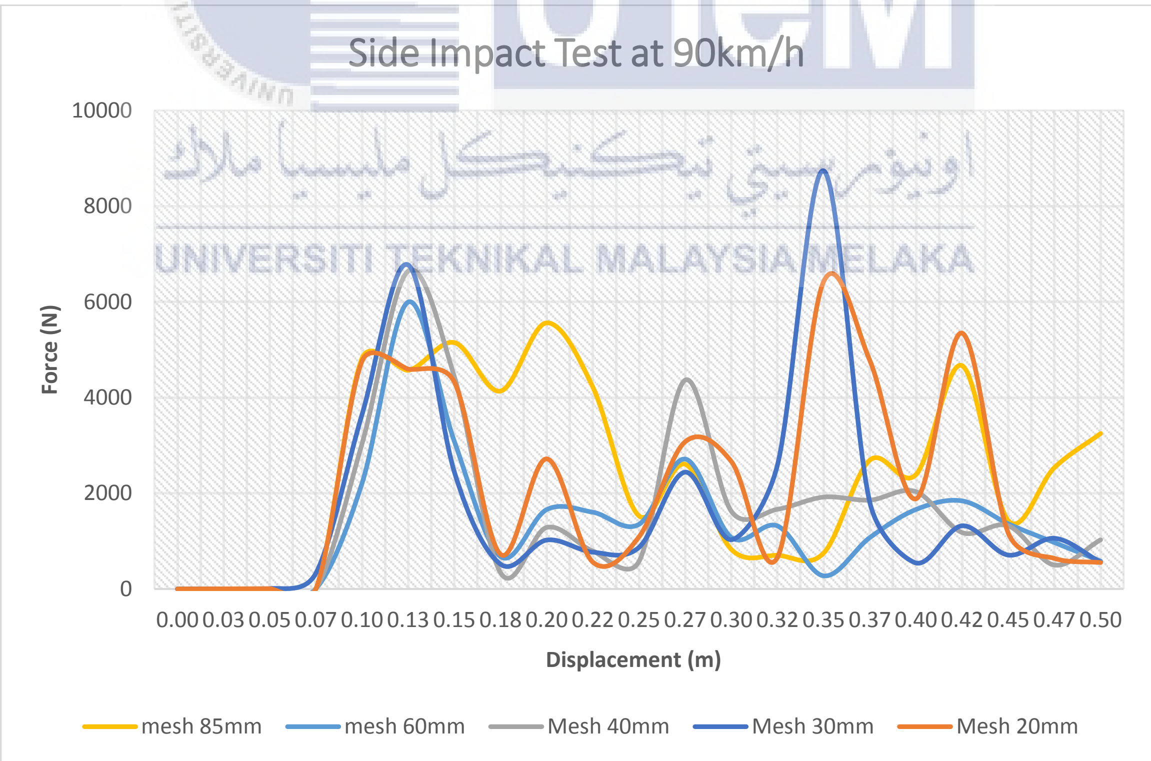

Figure 4.9: Force-displacement curves for side impact test with impact velocity of 90km/h

4.4 Rear Impact Test Simulation

Figure 4.10 shows the model assembly before the rear impact test simulation while Figure 4.11 shows deformed car roof structure after simulation. Since the bottom of car roof structure is fixed to the ground, the body deformed at the upper area of the rear roof structure, especially C-pillars. The average displacement of impactor in time span of 0.02s are 0.44m and 0.50m for 80km/h and 90km/h respectively. The displacement and reaction force at the striker are collected from nodes selected. The graphs of reaction force versus displacement for 80km/h and 90km/h are plotted as shown in Figure 4.12 and Figure 4.13 respectively.

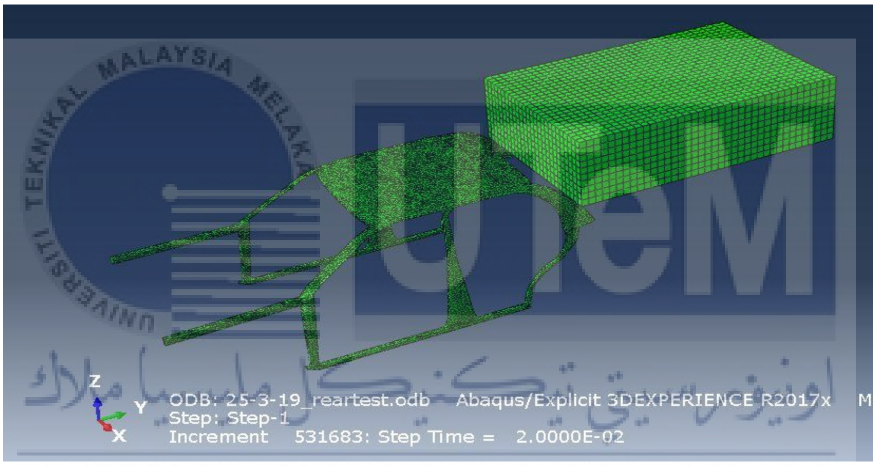

Figure 4.10 : Undeformed car roof structure before rear impact simulation

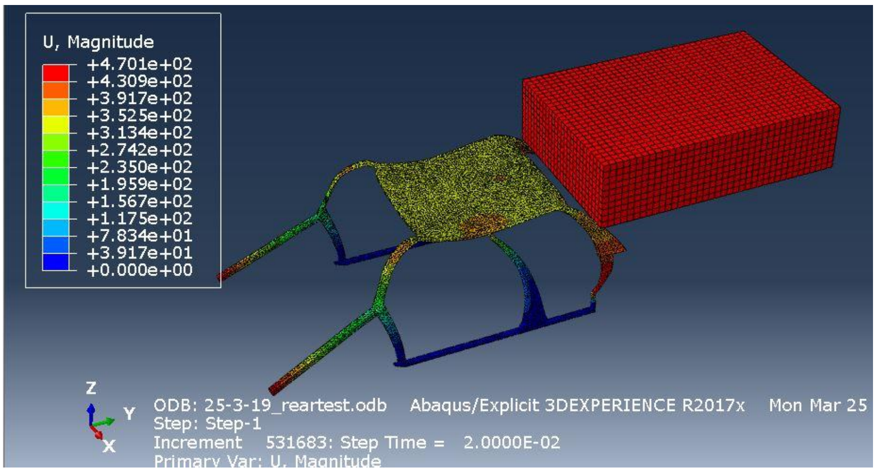

Figure 4.11 : Deformed car roof structure after rear impact simulation

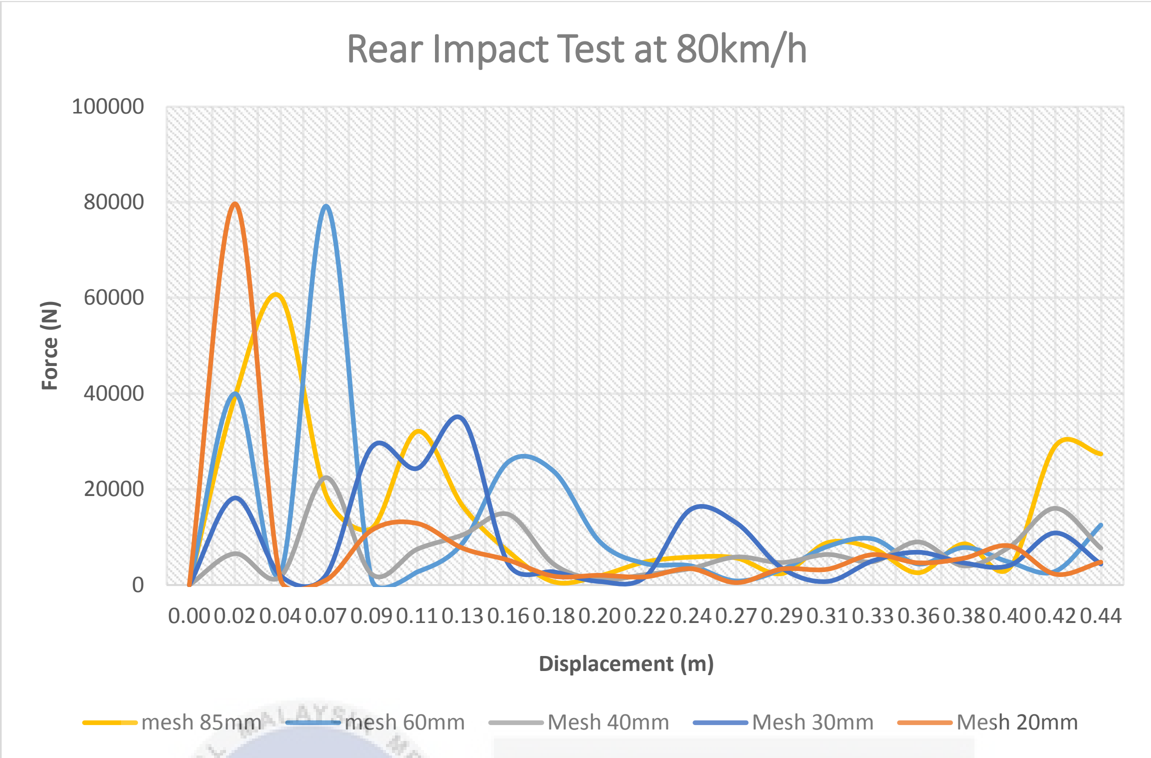

Figure 4.12: Force-displacement curves for rear impact test with impact velocity of 80km/h

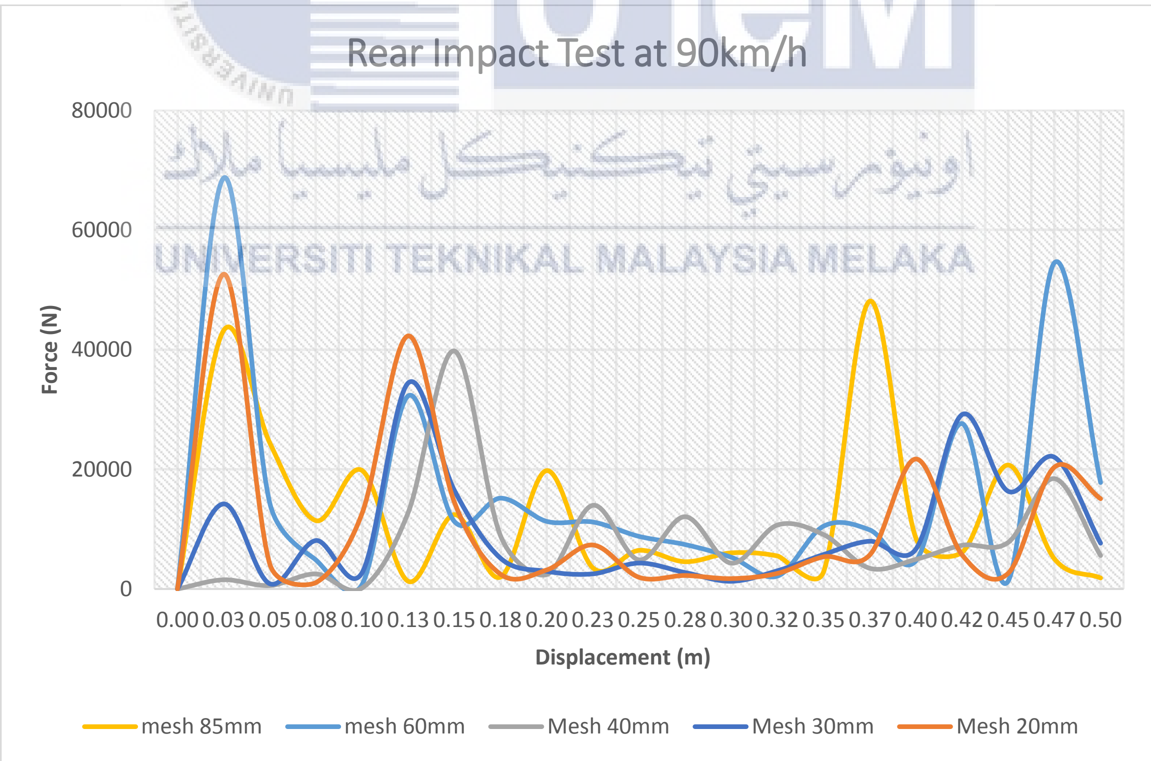

Figure 4.13: Force-displacement curves for rear impact test with impact velocity of 90km/h

4.5 Energy Absorbed

From the data collected, energy absorbed in each type of impact has been determined by the area under the force-displacement curve using Origin Pro software. The energy absorbed are recorded in Table 4.1 for frontal impact test, Table 4.2 for side impact test and Table 4.3 for rear impact test. Next, these pieces of information are presented in bar graphs as shown in Figure 4.14, Figure 4.16 and Figure 4.18 for a better visualization.

Table 4.1: Energy absorbed for frontal impact test with different impact velocities and different mesh sizes.

	Energy Absorbed (J)	
Impact Velocity (km/h) / Mesh Size (mm)	80	90
85	1904.30	3457.14
60	2624.06	2301.85
40	2673.91	2758.76
30	2863.14	2953.74
20	2922.54	3199.72

Table 4.2: Energy absorbed for side impact test with different impact velocities and different mesh sizes.

	Energy Absorbed (J)	
Impact Velocity (km/h) / Mesh Size (mm)	80	90
85	702.86	1257.92
60	354.21	728.43
40	546.93	852.51
30	618.51	923.23
20	652.15	1140.54

Table 4.3: Energy absorbed for rear impact test with different impact velocities and different mesh sizes.

	Energy Absorbed (J)	
Impact Velocity (km/h) / Mesh Size (mm)	80	90
85	6249.03	6310.27
60	5545.55	7775.36
40	3101.86	4213.13
30	4140.03	4780.00
20	3656.85	5433.39

Besides, to study the relationship between mesh size and energy absorbed, the percentage error is calculated by comparing the difference in result of each mesh size to the result of finest mesh (20mm) for each impact test with different impact velocity in this project. Percentage error of energy absorbed is calculated using Eq. (4.1) and the results are tabulated in Table 4.4, Table 4.5 and Table 4.6. For better visualisation, the information is translated into line graphs as shown in Figure 4.15, Figure 4.17 and Figure 4.19.

$$Percentage\ error\ (\%) = \frac{energy\ absorbed - energy\ absorbed\ of\ mesh\ 20mm}{energy\ absorbed\ of\ mesh\ 20mm} \times 100\% \qquad (4.1)$$

Table 4.4: Percentage error of energy absorbed in frontal impact test

	Percentage Error	
Impact Velocity (km/h) / Mesh Size (mm)	80	90
85	34.84%	8.05%
60	10.21%	28.06%
40	8.51%	13.78%
30	2.03%	7.69%
20	0%	0%

Table 4.5: Percentage error of energy absorbed in side impact test

	Percentage Error	
Impact Velocity (km/h) / Mesh Size (mm)	80	90
85	7.78%	9.33%
60	45.69%	36.13%
40	16.13%	25.25%
30	5.16%	19.05%
20	0%	0%

Table 4.6: Percentage error of energy absorbed in rear impact test

	Percentage Error	
Impact Velocity (km/h) / Mesh Size (mm)	80	90
85	70.89%	16.14%
60	51.65%	43.10%
40	15.18%	22.46%
30	13.21%	12.03%
20	0%	0%

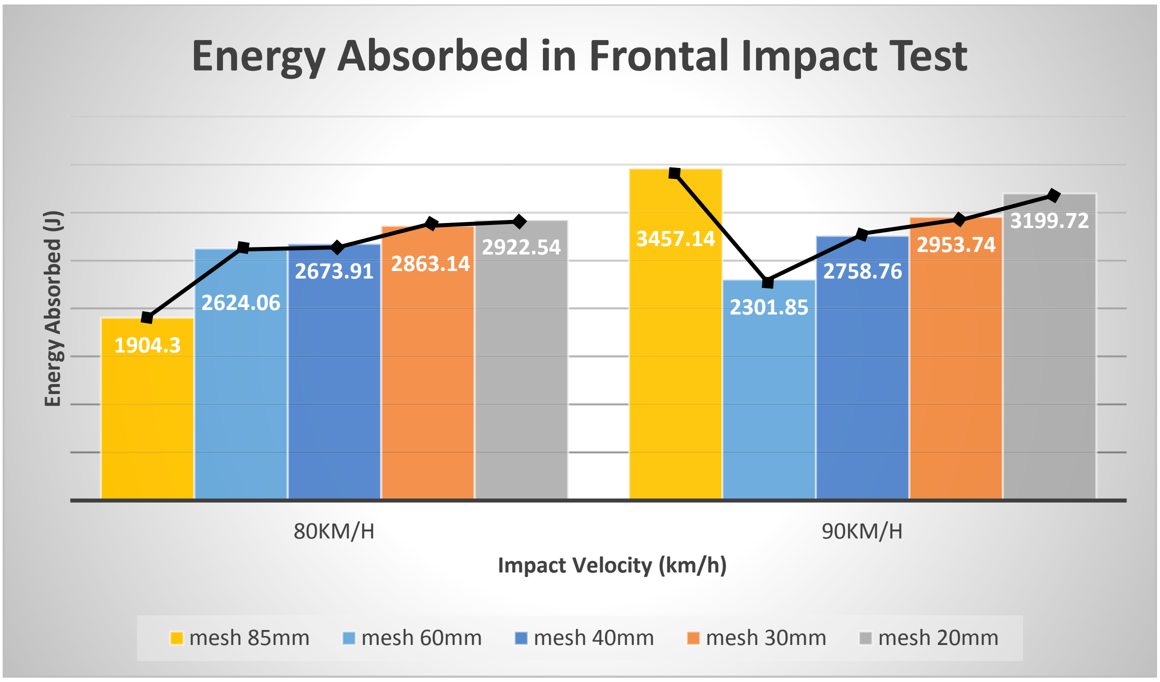

Figure 4.14: Energy absorbed for frontal impact test with different impact velocities and different mesh sizes.

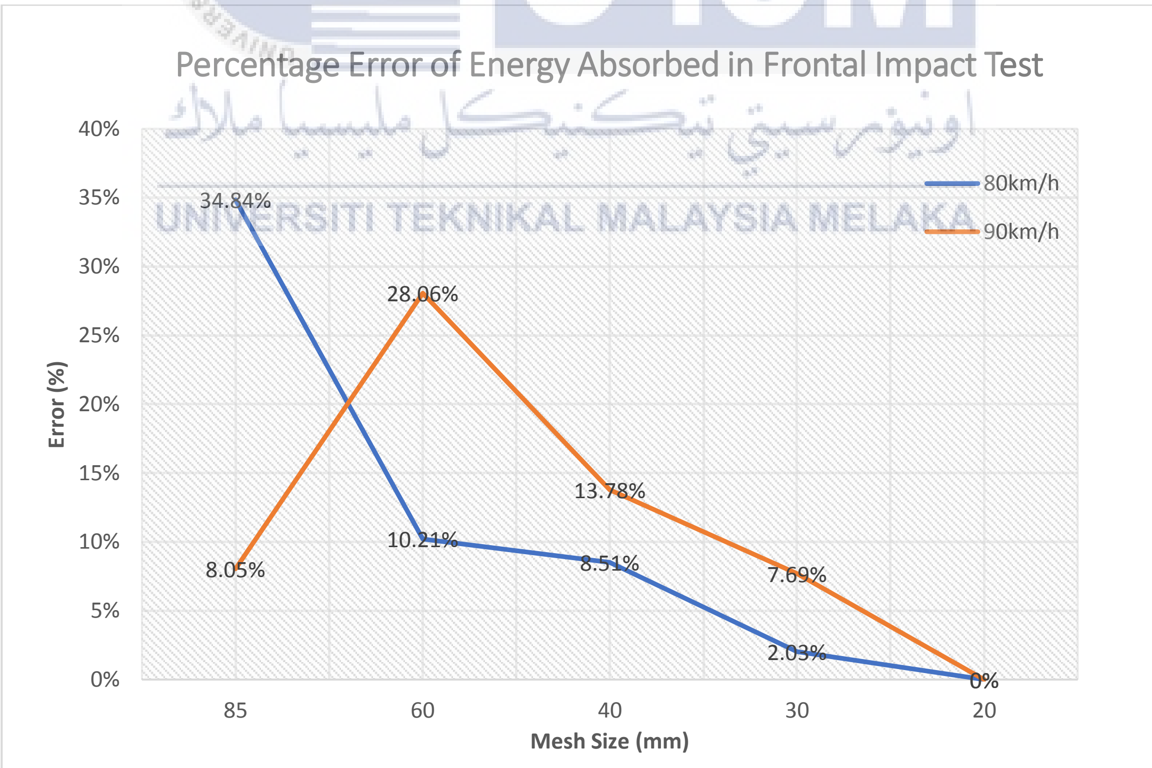

Figure 4.15: Percentage error of the energy absorbed for different mesh size for frontal impact test.

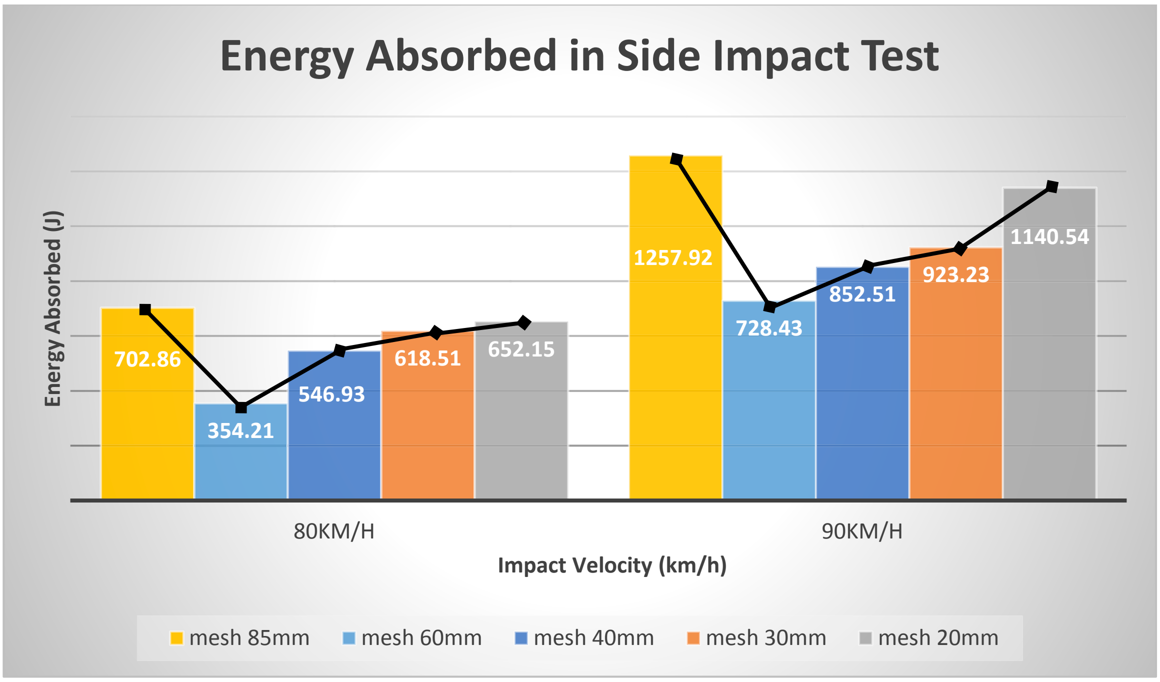

Figure 4.16: Energy absorbed for side impact test with different impact velocities and different mesh sizes.

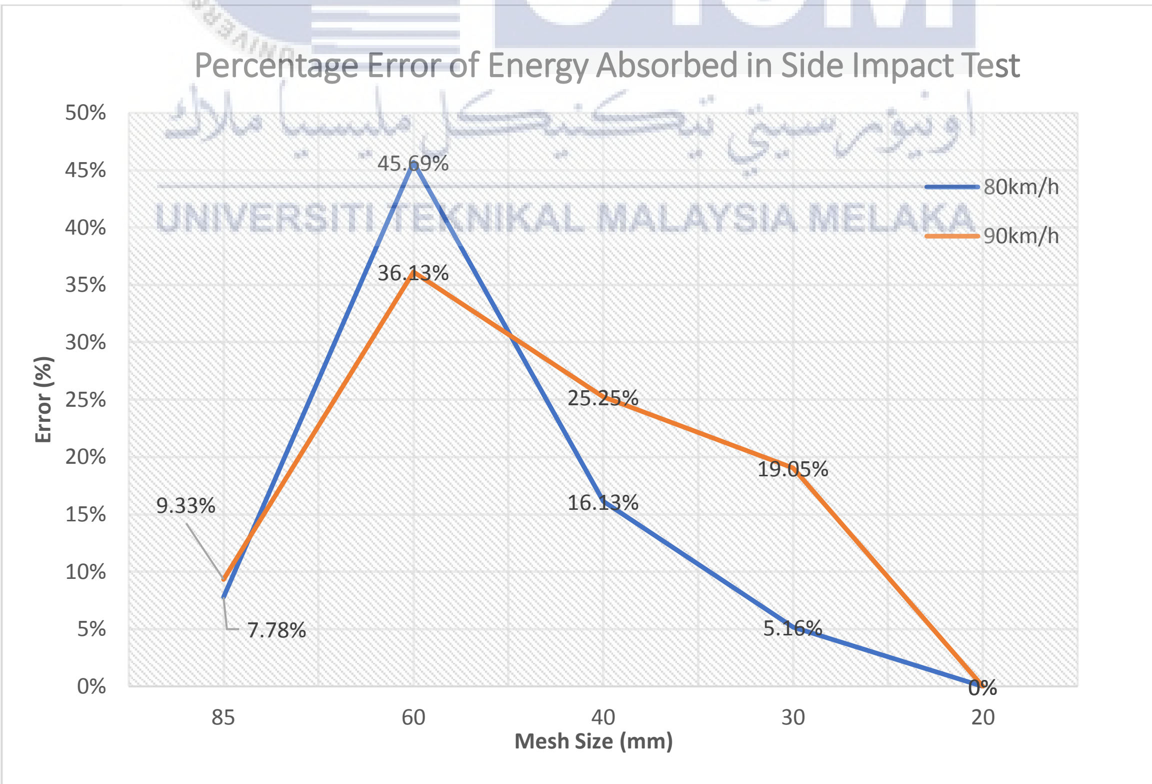

Figure 4.17: Percentage error of the energy absorbed for different mesh size for side impact test.

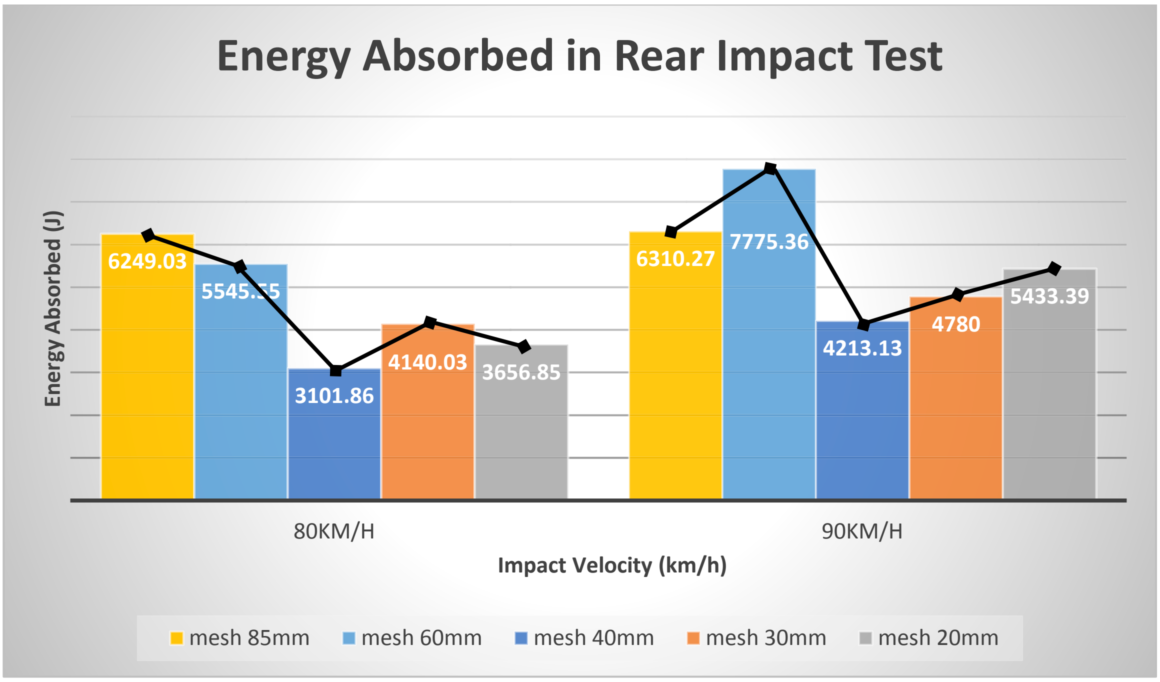

Figure 4.18: Energy absorbed for rear impact test with different impact velocities and different mesh sizes.

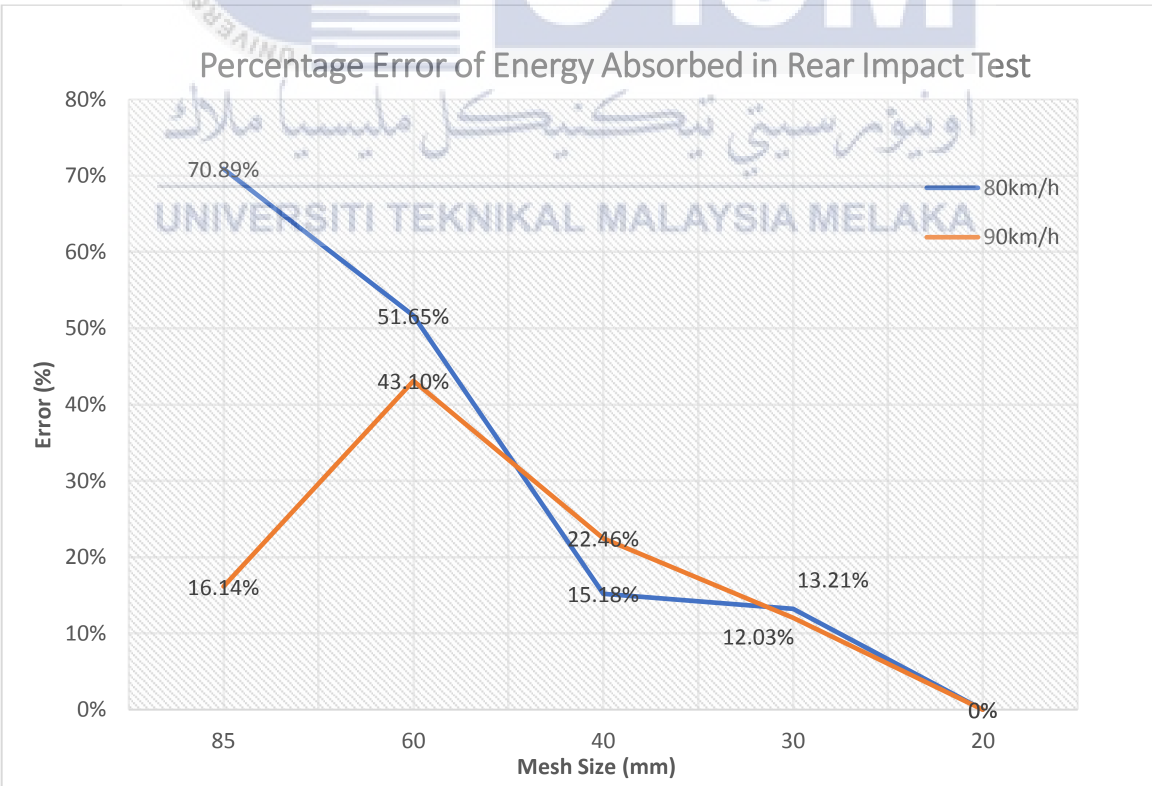

Figure 4.19: Percentage error of the energy absorbed for different mesh size for side impact

4.6 Discussion

According to the theory in FEA, smaller element size (fine mesh) will generate a relatively higher accuracy results if compares to the large element size (coarse mesh) (Liu and Glass, 2013). Therefore, the energy absorbed obtained from 20mm mesh size, the finest mesh in this project is expected to be the true value with little or no percentage error. From result of frontal impact test, as the mesh size decreasing from 85mm to 20mm, the energy absorbed is at an increasing trend for both 80km/h and 90km/h impact velocity. The same trend is found for side impact test except for the coarsest mesh; 85mm mesh which its energy absorbed is greater than that of the finest mesh for both 80km/h and 90km/h impact velocity. For rear impact test, energy absorbed does not have a constant increasing or decreasing trend as the mesh size decreases for both impact velocity. However, as the mesh size decreases, the value of energy absorbed become closer to each other, which means a relatively small difference.

From figures of percentage error of energy absorbed as shown in Figure 4.15, Figure 4.17 and Figure 4.19, as meshing size decreases, the percentage error of the result also decreases. In frontal impact test, the percentage error of energy absorbed in both 80km/h and 90km/h are converged to 2.03% and 7.69% as the mesh size decreased to 30mm. For side impact test, this value is 5.16% and 19.05% for impact velocity of 80km/h and 90km/h respectively. Surprisingly, for 85mm mesh in side impact test, the percentage error is very low; 7.78% and 9.33% for 80km/h and 90km/h respectively. However, the percentage error surged to 45.69% and 36.13% as mesh size decreased to 60mm, then dropped all the way as mesh size decreased further to 40mm, 30mm and 20mm. Next, percentage error in rear impact test is 13.21% and 12.03% respectively for 30mm mesh. The highest percentage error across all simulation is 70.89% at 85mm mesh for 80km/h in rear impact test. Therefore, it can be said that the percentage error of the value of energy absorbed is decreasing with mesh size.

By validated and verified the result from 20mm mesh as the most precise value, the energy absorbed for each impact test with different impact velocity is concluded. In frontal impact test, the energy absorbed by car roof is 2922.54J for an impact velocity of 80km/h and increased to 3199.72J for 90km/h. In side impact test, the energy absorbed during an impact velocity of 80km/h is determined as 652.15J and escalated to 1140.54J when impact velocity increased to 90km/h. For rear impact test, 3656.85J is determined as the energy absorbed by the car roof during the 80km/h impact test and surged to 5433.39J as the impact velocity raised to 90km/h. From all type of impact test, it can be concluded that the energy absorbed by car roof structure in 90km/h is generally higher than that of 80km/h regardless of which mesh size expect for mesh 60mm in frontal impact test. From theory, as impact velocity increased, the force increased, and therefore energy absorbed will increase too (Mujahid *et al.*, 2010). Therefore, this theory is justified in this project.

By comparing the results obtained, energy absorbed by the car roof structure during the impact is the highest for rear impact, followed by frontal impact and the smallest for side impact test. This implies C-pillar can absorb more energy when the truck impacts with the car from the rear side of the car. Next, A-pillars can absorb the second most energy when the truck crash into the frontal side of the car if compared to B-pillars and C-pillars. Last but not least, B-pillar that situated at the side of the car absorbs relatively less amount of energy comparing to other pillars. This might due to the thickness of the car roof pillars. The thickness of car roof pillars is in ascending order from B-pillar (side) to A-pillar (front) and to C-pillar (rear). Thus, when the thickness of car roof pillars increased, more kinetic energy can be absorbed. This result gives a good agreement with the theory on the energy absorption which states that energy absorption capability increasing with wall thickness (Mujahid *et al.*, 2010). Besides, the lowest energy absorbed during side impact also due to relatively little space to absorb energy at the sides of vehicles (Reichert, R., Kan, Arnold-Keifer and Mueller, 2018).

From the result of this project, concluded that the current design of roof structure is not likely to prevent fatality in an underride crash alone that involved a truck and a passenger car for impact velocity at 80km/h and 90km/h. The energy absorbed by the roof structure is range from 652.15J to 3656.85J for 80km/h, 1140.54J to 5433.39J for 90km/h. By using Equation 1, the impact energy generated during the impact are calculated and gathered in Table 4.7. Only about 0.1% of the total impact energy generated is absorbed by the car roof structure.

Table 4.7: Impact energy generated during the impact for different impact velocity

Impact Velocity (km/h)	Impact Energy (KJ)
80	3950
90	5000

All result from this project is simulated in a way that the crash is to be taken place at 0.02s by set the step time for all simulation as 0.02s in ABAQUS software. To know the significance of the result from this project, author have done extra simulations of frontal impact test by using longer step time; 0.03s and 0.05s to simulate a longer crashing event using impact velocity of 80km/h to see the variation in term of displacement and energy absorbed. The screenshots of the deformed car roof structure obtained from the result of extra simulations are shown in Figure 4.20.

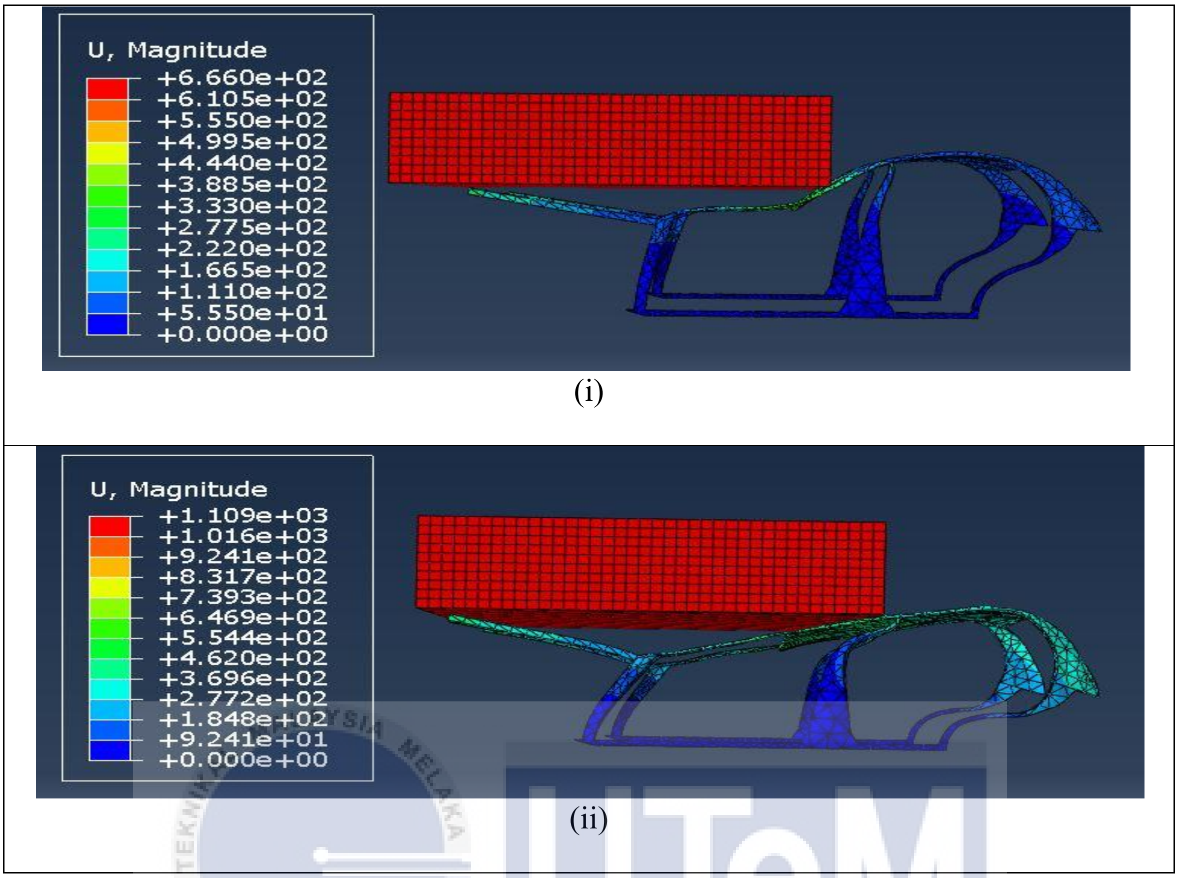

Figure 4.20: Frontal impact test at impact velocity of 80km/h for different step time; (i) 0.03s, (ii) 0.05s

From Figure 4.20, the maximum displacement for the impactor is 0.66m for step time of 0.03s and increased significantly to 1.10m for step time of 0.05s. Also, from the data extracted, the energy absorbed is determined as 8597.61J and 23244.04J for 0.03s and 0.05s step time respectively. As time of impact increase, more energy is absorbed. However, it still account for a very small percentage (0.2%-0.5%) of the impact energy generated during the crash. If this scenario happens in real-world, the passengers in the car will not be able to survive due to excessive passenger compartment intrusion (PCI). For this project, the impactor which is the model of the truck is generated without underride guards. Thus, it is very obvious that the car roof is not able to absorb a big portion of kinetic energy that generated during the crash alone without the presence of underride guards installed on trucks.

This study reveals the reason why is that the main focus is on the truck side for safety measures for underride crash especially the underride guards. Nowadays, underride guards installed on trucks are capable to provide high levels of occupant protection up to 56 km/h. However, optimisation on the strength of car roof to absorb more impact energy to cope with the underride guards of truck is worth for a further study to improve the overall energy absorption capability to save more life from underride crashes.

CHAPTER 5

CONCLUSION AND RECOMMENDATIONS FOR FUTURE RESEARCH

5.1 Conclusion

The literature study is to investigate the strength of car roof structure in term of energy absorption in an impact test by using CATIA and Abaqus software. From literature review done in chapter 2, concluded that there is virtually no any study on the strength of car roof but almost all researches are on the underride guards that installed on large vehicle when comes to safety measure of underride crash. Therefore, this project is to study on the crashworthiness of the passenger car roof pillars when underride crash happens involved of small passenger car and a larger vehicle such as truck or trailer.

The strength of car roof is crucial in an underride crash because it is the impact area between both vehicles surpass the crumple zone. This is because when the underride guards which installed on the truck fails, the energy absorption will be solely depends on the smaller car itself. The strength of car roof is defined by how well it can absorb the energy during the impact and reduce the injuries and fatalities to the car's occupants because of less PCI.

In this study, the objectives of this project are achieved. First of all, the objective to improve the design of 3D model for real car roof by adding body structure to the car roof. This objective is achieved by redesigned the real car roof structure using CATIA software based on the real dimensions measured from PROTON WIRA. The 3D model retrieved from previous study was unusable because many errors was found such as dimensions and type of modelling used. Next, the second objective of this project; to determine the energy absorbed on different side of car roof (front, rear, side) during the impact is achieved. This objective is achieved by conducting Finite Element Analysis (FEA) for the impact simulation of car roof structure in different orientation using ABAQUS software. The energy absorbed is increased in the order from side to front and to the largest on the rear side of the roof structure as determined from the result of simulations.

5.2 Recommendation for Future Research

For every FEA simulation, the 3D model for simulation is the most crucial element to produce a reliable result of test data. In another word, for the result generated to be "correct", the model must be "correct". Therefore, verification and validation of 3D model need to be conducted to determine the model validity. However, it is not easy to verify and validate the model because this project presents a new test that never been conducted before. Some of the validation techniques include comparison to other models and comparison to experimental data obtained from real-world model. It is not economical to perform real impact test due to its high cost. Therefore, it is recommended the results obtained from this study is compared to similar car model that redesign by the next researcher. The model and result then can be validated through comparison of both test data obtained from FEA.

In addition, for this project, the simulation time taken for 20mm mesh is about 2 days to complete. By further decreasing the mesh size to 10mm, it was found that the time required to complete the simulation escalated to about 7days. Due to time constraint in this project, the finest mesh size used is up to maximum of 20mm only. Therefore, second recommendation is that the simulation should be continued with car roof structure of finer mesh size such as 10mm, 5mm and so on. With the result obtained from these finer mesh sizes, we can further verify the "correctness" of energy absorbed. If the result does converge to a certain value as the mesh size decreases, then the value which it is converging is judged as the true value.

Last but not least, the model of impactor can be improved by modelling it into more details. Future research should include the underride guards in this study in order to determine the energy absorbed by the car roof structure more accurately. Different type of trucks or lorry with different weight can be simulated to impact with the car roof structure to determine the energy absorbed in each case since there are many types of trucks on the roads.

REFERENCES

(NHTSA), N. H. T. S. A. (1989) 'Laboratory test procedure for FMVSS 216 - Roof crush resistance -- Passenger cars', TP-216-04, pp. 1–40.

Abdel-Nasser, Y. A. (2013) 'Frontal crash simulation of vehicles against lighting columns using FEM', *Alexandria Engineering Journal*. Faculty of Engineering, Alexandria University, 52(3), pp. 295–299. doi: 10.1016/j.aej.2013.01.005.

Ali, M. B. *et al.* (2011) 'Evaluating charpy impact signals using power spectrum densities: A finite element method approach', *International Journal of Mechanical and Materials Engineering*, 6(1), pp. 92–101.

Ambati, T., Srikanth, K. and Veeraraju, P. (2012) 'Simulation of vehicular frontal crashtest', *International Journal of Applied Research in Mechanical Engineering (IJARME)*, 2(1), pp. 37–42.

ArcelorMittal (2010) 'Steels for hot stamping, Product Catalog'.

ASEAN NCAP (2017) 'ASSESSMENT', *NEW CAR ASSESMENT PROGRAM FOR SOUTHEAST ASIAN COUNTRIES (ASEAN NCAP) OVERALL ASSESSMENT PROTOCOL*, (January), pp. 0–8.

Balta, B. *et al.* (2014) 'Pareto Optimization of Heavy Duty Truck Rear Underrun Protection Design for Regulative Load Cases', *SAE International Journal of Commercial Vehicles*, 7(2), pp. 2014-01–9027. doi: 10.4271/2014-01-9027.

Bloch, B. *et al.* (no date) 'Improved crashworthy designs for truck underride guards'.

Bodapati, V. K. K. (2004) 'Evaluation of Energy Absorbing Pliers Underride Guards for', (December).

Bois, P. D. *et al.* (2004) *Vehicle crashworthiness and occupant protection*, *American Iron and Steel Institute*. doi: 10.1121/1.2783205.

Borazjani, S. and Belingardi, G. (2017) 'Development of an innovative design of a composite-sandwich based vehicle roof structure', *Composite Structures*, 168, pp. 522–534. doi: 10.1016/j.compstruct.2017.02.015.

Breu, F., Guggenbichler, S. and Wollmann, J. (2008) 'Performance of Large Truck Rear Underride Guard', *Proceedings of the*, (11), pp. 1–8. Available at: http://medcontent.metapress.com/index/A65RM03P4874243N.pdf.

Car Safety Features and Systems (no date). Available at: https://sites.google.com/site/carsafetyfeaturesandsystems/crumple-zones (Accessed: 10 December 2018).

Chang, C. L. and Yang, S. H. (2009) 'Simulation of wheel impact test using finite element method', *Engineering Failure Analysis*, 16(5), pp. 1711–1719. doi: 10.1016/j.engfailanal.2008.12.010.

Chen, T. *et al.* (2007) 'Rollover far side roof strength test and simulation', *International Journal of Crashworthiness*, 12(1), pp. 29–39. doi: 10.1533/ijcr.2006.0156.

Cofaru, C. (2015) 'Study of Current State of Crash Testing', 8(2).

Conroy, C. *et al.* (2006) 'Rollover crashes: Predicting serious injury based on occupant, vehicle, and crash characteristics', *Accident Analysis and Prevention*, 38(5), pp. 835–842. doi: 10.1016/j.aap.2006.02.002.

Costas, M. *et al.* (2013) 'International Journal of Impact Engineering Static and dynamic axial crushing analysis of car frontal impact hybrid absorbers', 62, pp. 166–181.

Crashes, I. *et al.* (1991) *Truck Involved Crash Study Report on :*

Dobbertin, K. M. *et al.* (2013) 'The relationship between vehicle roof crush and head, neck and spine injury in rollover crashes', *Accident Analysis and Prevention*, 58, pp. 46–52. doi: 10.1016/j.aap.2013.04.020.

Duane Bong (no date) 'Crumple Zones'. Available at: https://studylib.net/doc/7842661/crumple-zones-reading-and-questions.

EFunda (no date) *Properties of Boron Alloy Steel*. Available at: http://www.efunda.com/Materials/alloys/alloy_steels/show_alloy.cfm?ID=AISI_4140&prop=all&Page_Title=AISI 4140.

Friedman, D. and CE, N. (2001) 'Advanced roof design for rollover protection', *Advanced roof design for rollover protection*, 01-S12-W-9, pp. 1–10.

Gohlami, T., Lescheticky, J. and Paßmann, R. (2003) 'Crashworthiness simulation of automobiles with ABAQUS/Explicit', *Proceeding of Abaqus Users' Conference, June Munich*, pp. 1–18.

Grimolizzi, E. and Cravotta, S. C. (2015) 'Simulation of vehicle impact into a steel building A PARAMETRIC STUDY ON THE IMPACTED COLUMN END-CONNECTIONS SCHOOL OF ARCHITECTURE AND THE BUILT ENVIRONMENT'. Available at: http://kth.diva-portal.org/smash/get/diva2:847125/FULLTEXT01.pdf.

Grzebieta, R., Mcintosh, A. and Simmons, K. (2012) 'Kennerly Digges', *National Crash Analysis Center*, (13–0098), pp. 1–9.

Hs, D. O. T. (2013) 'Heavy-Vehicle Crash Data Collection And Analysis to Characterize Rear and Side Underride and Front Override in Fatal Truck Crashes', (March).

https://qbtransportation.com (2018) *53' sheet & post van*.

https://www.heavydutydirect.ca/need-to-know-about-dry-van-trailers (2018) *Types of Dry Van Trailers Uses of Dry Van Trailers Other facts about Dry Van HOME Trailers*.

IIHSA (2016) 'Federal Motor Vehicle Safety Standards 49 CFR Part 571, Rear Impact Guards, Rear Impact Protection; Notice of Proposed Rulemaking; Docket No. NHTSA-2015-0118 Dear', pp. 31–48.

Insurance Institute for Highway Safety, Highway Loss Data Institute (no date) *Insurance Institute for Highway Safety*. Available at: https://www.iihs.org/iihs/ratings/ratings-info/frontal-crash-tests (Accessed: 9 November 2018).

Jawi, Z. M., Kassim, K. A. A. and Sadullah, A. F. (2013) 'ASEAN NCAP–The Best Bet for Vehicle Safety in the Region's Safe System?', *International Journal of Trade, Economics and Finance*, 4(6), pp. 358–363. doi: 10.7763/IJTEF.2013.V4.317.

Kamruzzaman, S. (2000) *Energy absorption of tubular structures*. Available at: http://repositories.tdl.org/tdl-ir/browse?order=DESC&rpp=100&sort_by=2&etal=-1&offset=15656&type=dateissued.

Kumar, G. D. L. *et al.* (2018) 'Crash Analysis of four wheel vehicle for different velocity', pp. 1530–1538.

Liu, Y. and Glass, G. (2013) 'Effects of Mesh Density on Finite Element Analysis', *SAE Technical Paper Series*, 1. doi: 10.4271/2013-01-1375.

Ministry Of Transport Malaysia (no date) *Index of Accidental Road Death*. Available at: http://www.mot.gov.my/en/lands/public safety-roads/statistics-accidents-jalan-raya-index-death (Accessed: 25 October 2018).

Mohd Syazwan, S. *et al.* (2014) 'ASEAN NCAP Crash Tests: Modifier Assessment Justified', *Applied Mechanics and Materials*, 663, pp. 547–551. doi:

10.4028/www.scientific.net/AMM.663.547.

MUHAMMAD AFIFUDDIN (2018) ‘IMPACT TEST SIMULATION USING FINITE ELEMENT ANALYSIS (FEA) FOR CAR ROOF’.

Mujahid, A. *et al.* (2010) ‘Numerical Simulation Study on Lateral Collapse of Kenaf-Foam Composite Filled in Cylindrical Tube Subjected to Dynamic Loading’, pp. 97–110.

NHTSA (2015a) ‘PRELIMINARY REGULATORY EVALUATION FMVSS No . 223 and FMVSS No . 224’, (224).

NHTSA (2015b) ‘Rear Impact Guards, Rear Impact Protection’, 80(132), pp. 1–25.

Njuguna, J. (2011) ‘The Application of Energy Absorbing Structures on Side Impact Protection Systems’, 40(4).

Park, B. T. *et al.* (1998) ‘Frontal offset crash test study’, pp. 150–163.

Physics, T. and Collision, C. (2018) *The Physics of a Car Collision Energy and force are involved in the crash*. Available at: https://www.thoughtco.com/what-is-the-physics-of-a-car-collision-2698920.

Reddy, N. (2013) ‘Study of Different Parameters on the Chassis Space Frame For the Sports Car by Using Fea’, *IOSR Journal of Mechanical and Civil Engineering*, 9(1), pp. 01–09. doi: 10.9790/1684-0910109.

Reichert, R., Kan, S., Arnold-Keifer, S. and Mueller, B. (2018) ‘IIHS Side Impact Parametric Study using LS-DYNA ®’, pp. 1–12.

Road Safety Department and Malaysian Institute of Road Safety Research (2014) *Road Safety Plan Of Malaysia 2014-2020*. doi: 10.1088/0741-3335/51/5/055015.

Roberts, G. L. and Lynn, C. W. (2003) *Contract Report Passenger Vehicle Crashes Into*

Stationary Large Trucks : Incidence and Possible Countermeasures, *PASSENGER VEHICLE CRASHES INTO STATIONARY LARGE TRUCKS: INCIDENCE AND POSSIBLE COU NTERMEASURES*.

Shenoy, S. S. and Lankarani, H. M. (2006) 'Energy absorption of a car roof reinforced with a grid stiffened composite panel in the event of a rollover', *Energy absorption of a car roof reinforced with a grid stiffened composite panel in the event of a rollover*, 1441978(May), pp. 80-80 p. Available at: http://search.proquest.com/docview/304978627?accountid=43623.

Sherwood, C. P. *et al.* (2013) 'Development of a Frontal Small Overlap Crashworthiness Evaluation Test', *Traffic Injury Prevention*, 14(SUPPL1). doi: 10.1080/15389588.2013.790539.

Thakur, R. and NATALE, A. (2009) 'Federal Motor Vehicle Safety Standards; Roof Crush Resistance; Phase-In Reporting Requirements', *Cardiology Clinics*, 27(1), pp. xv–xv.

Types of Collisions (2018). Available at: http://ffden-2.phys.uaf.edu/211_fall2002.web.dir/ben_townsend/TypesofCollisions.htm.

WHO (2008) *Speed management: a road safety manual for decision-makers and practitioners.* doi: 10.1787/9789282103784-en.

Wishdom, W. (2018) *Pillars of your car*. Available at: https://www.wheelswisdom.com/blogs/car-driving/your-cars-pillars-of-support/.

Yang, N. *et al.* (2016) 'Crashworthiness optimisation of A-pillar in passenger car in rear-end collision with truck', *International Journal of Crashworthiness*, 21(6), pp. 507–520. doi: 10.1080/13588265.2016.1192087.

Yusak, N. F. B. M. (2018) 'Weight Restriction Order (Amendment) 2003', pp. 1–5.

Zainuddin, H. *et al.* (2016) ‘Correlation between vertical wheel impact energy with lateral wheel impact energy: A finite element analysis approach’.

APPENDIX

A. Technical drawing of the car roof model

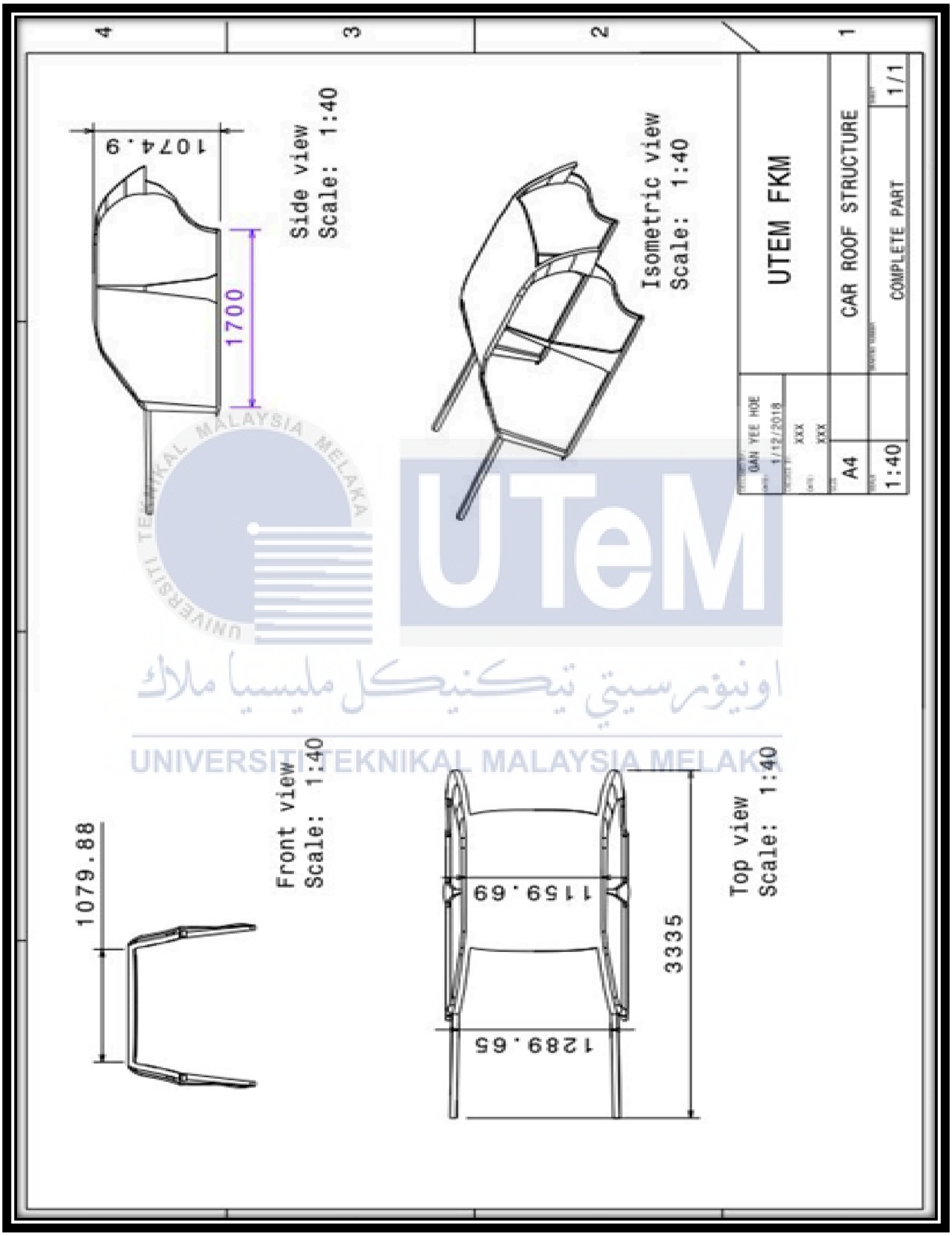

Figure A: Technical drawing of car roof model

B. Dimension of 2015 Vanguard dry van semi-trailer – reference for ratio of length, width and height of the impactor created in this project

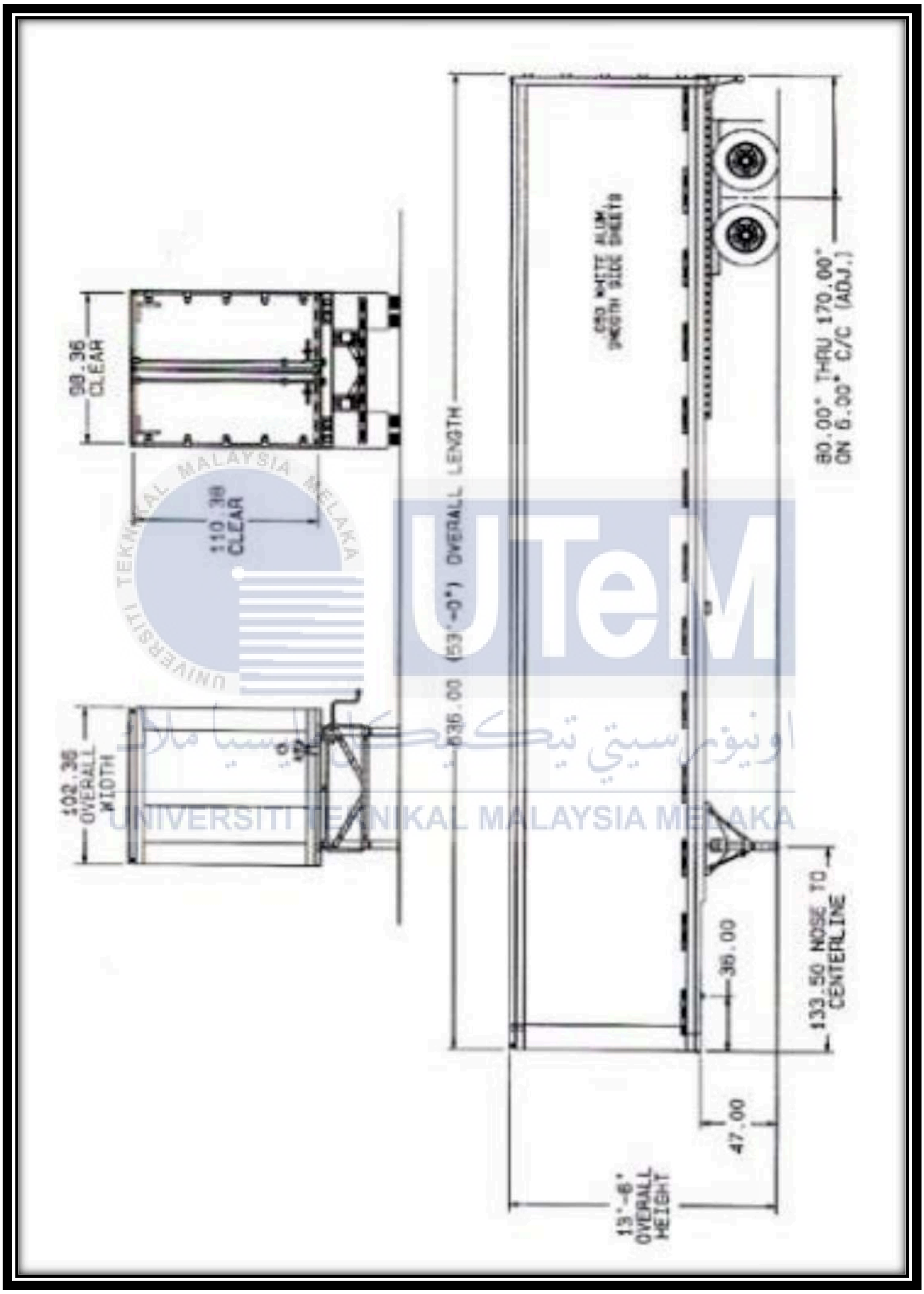

Figure B: The dimensions of the 2015 Vanguard dry van semi-trailer (https://qbtransportation.com, 2018)

C. Results of ABAQUS simulation for frontal impact test on car roof structure

Table C1: Frontal impact test with different mesh size for different impact velocity

<table>
<tr><td></td><td colspan="2">Frontal Impact Test</td></tr>
<tr><td></td><td>80km/h</td><td>90km/h</td></tr>
<tr><td>A</td><td>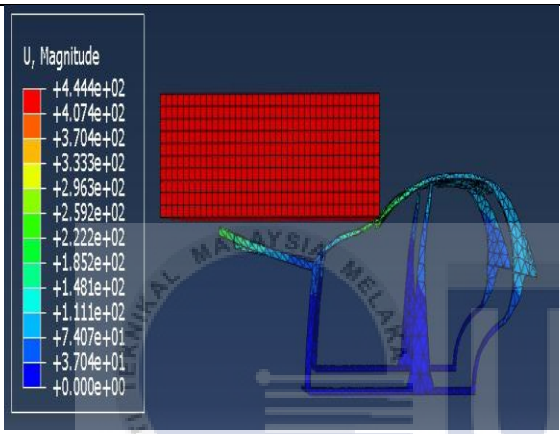
</td><td>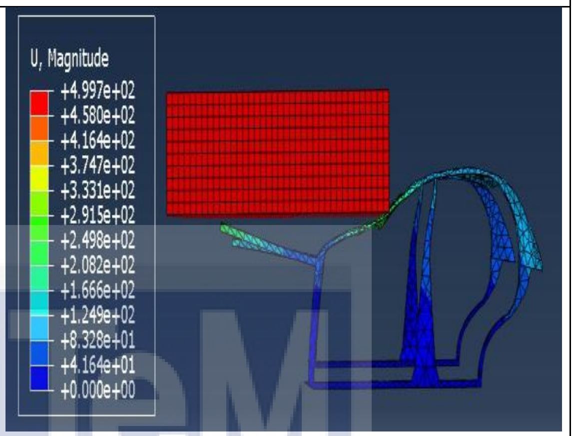
</td></tr>
<tr><td>B</td><td>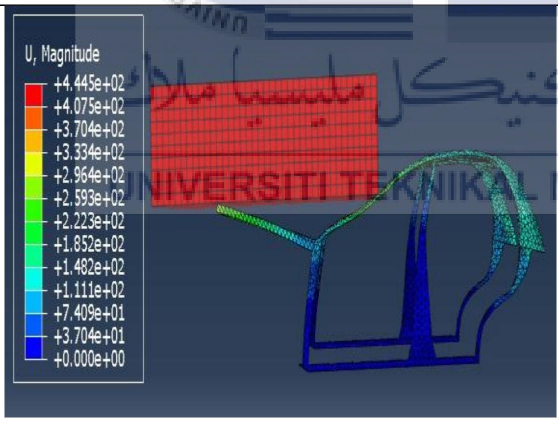
</td><td>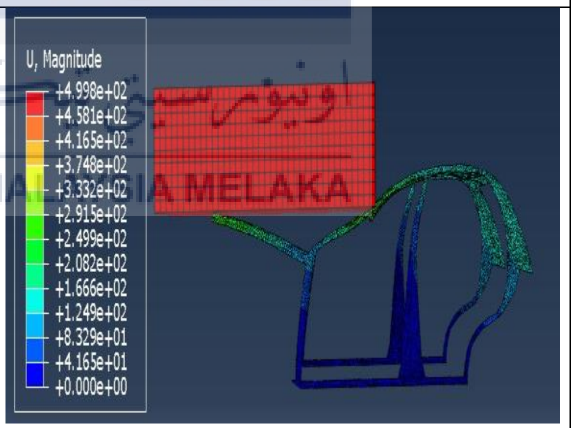
</td></tr>
</table>

A: 85mm mesh (coarse mesh)

B: 20mm mesh (fine mesh)

D. Results of ABAQUS simulation for side impact test on car roof structure

Table D1: Side impact test with different mesh size for different impact velocity

<table>
<tr><td></td><td colspan="2">Side Impact Test</td></tr>
<tr><td></td><td>80km/h</td><td>90km/h</td></tr>
<tr><td>A</td><td>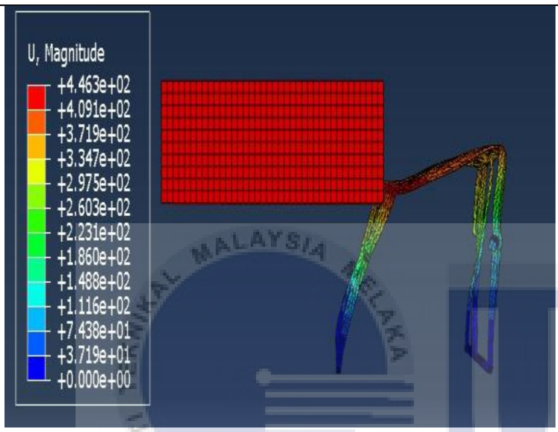
</td><td>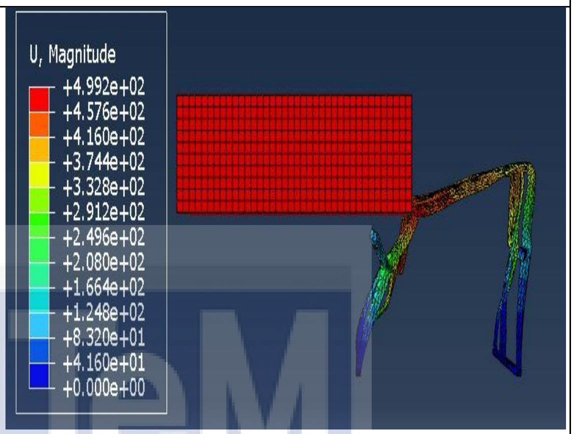
</td></tr>
<tr><td>B</td><td>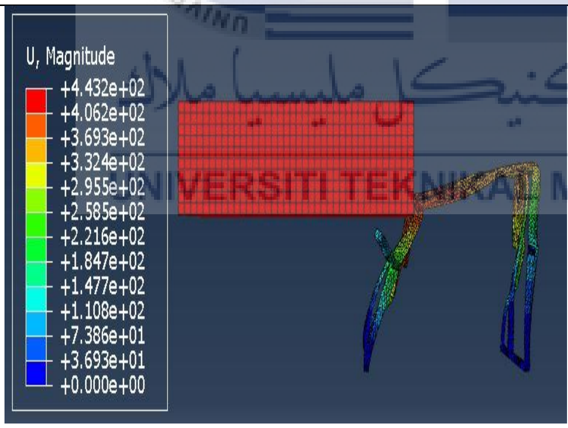
</td><td>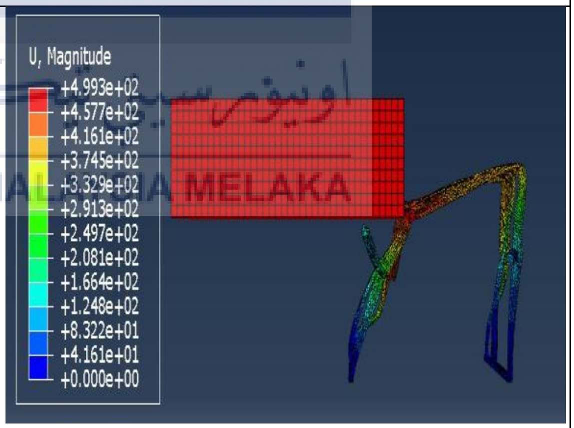
</td></tr>
</table>

A: 85mm mesh (coarse mesh)

B: 20mm mesh (fine mesh)

E. Results of ABAQUS simulation for rear impact test on car roof structure

Table E1: Rear impact test with different mesh size for different impact velocity

	Rear Impact Test	
	80km/h	90km/h
A	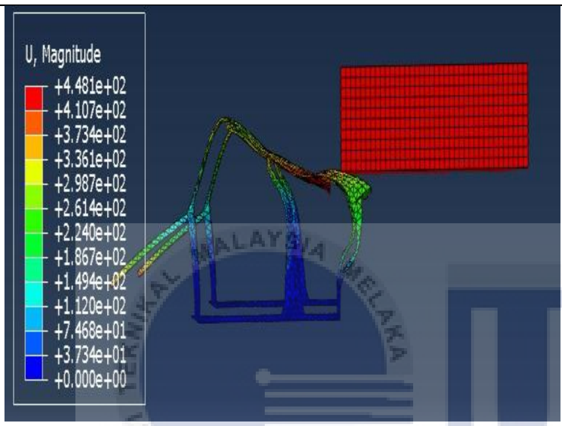	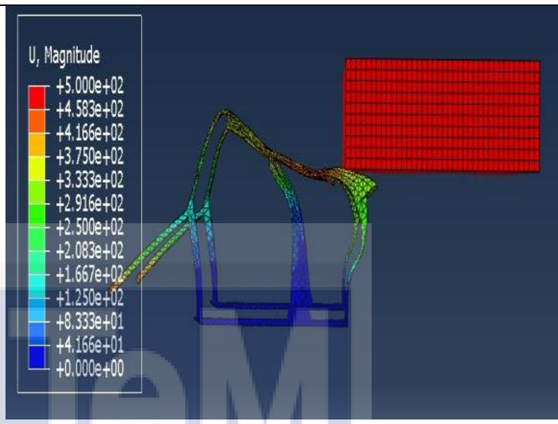
B	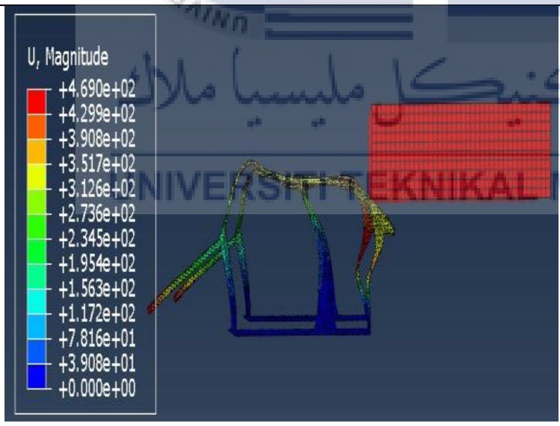	

A: 85mm mesh (coarse mesh)

B: 20mm mesh (fine mesh)